Timing and development of sedimentation of the Cleaverville Formation and a post-accretion pull-apart system in the Cleaverville area, coastal Pilbara Terrane, Pilbara, Western Australia

Kiyokawa, Shoichi
Department of Earth and Planetary Science, Kyushu University

Aihara, Yuhei
Department of Earth and Planetary Science, Kyushu University

Takehara, Mami
National Institute of Polar Research

Horie, Kenji
National Institute of Polar Research

出版情報：Island Arc. 28 (6), pp.e12324-, 2019-09-15. Wiley
バージョン：
権利関係：

Timing and development of sedimentation of the Cleaverville Formation and a post-accretion pull-apart system in the Cleaverville area, coastal Pilbara Terrane, Pilbara, Western Australia

Shoichi Kiyokawa[a,b,c], Yuhei Aihara[a,d], Mami Takehara[e], Kenji Horie[e,]

[a] Department of Earth and Planetary Science, Kyushu University, 744 Motooka Nishiku, Fukuoka 819-0395, Japan

[b] Department of Geology, University of Johannesburg, PO Box 524 Auckland Park, Johannesburg, 2006, South Africa

[c] Kochi Marine Core Center, Kochi University, Nankoku, Kochi, Japan

[d] INPEX CORPORATION, Akasaka Biz Tower 5-3-1 Akasaka, Minato-ku, Tokyo 107-6332, Japan

Current address

[e] National Institute of Polar Research, 10-3, Midori-cho, Tachikawa-shi, Tokyo 190-8518, Japan

E-mail addresses

Shoichi Kiyokawa: kiyokawa@geo.kyushu-u.ac.jp Tel.: 092-802-4254

Corresponding author:

Yuhei AIHARA: sstibnite@gmail.com

Kenji HORIE: horie.kenji@nipr.ac.jp

Mami TAKEHARA: takehara.mami@nipr.ac.jp

Abbreviated article abstract

The Cleaverville Formation was deposited at ca. 3.1 Ga.

A strike-slip pull-apart basin formed in the Cleaverville area at 2.93 Ga.

Abstract

In the Cleaverville area of Western Australia, the Regal, Dixon Island, and Cleaverville Formations preserve a Mesoarchean lower-greenschist-facies volcano-sedimentary succession in the coastal Pilbara Terrane. These formations are distributed in a rhomboidal-shaped area and are unconformably overlain by two narrowly distributed shallow-marine sedimentary sequences: the Sixty-Six Hill and Forty-Four Hill Members

of the Lizard Hills Formation. The former member is preserved within the core of the Cleaverville Syncline and the latter formed along the northeast-trending Eighty-Seven Fault. Based on the metamorphic grade and structures, two deformation events are recognized: D_1 resulted in folding caused by a collisional event, and D_2 resulted in regional sinistral strike-slip deformation. A previous study reported that the Cleaverville Formation was deposited at 3020 Ma, after the Prinsep Orogeny (3070–3050 Ma). Our SHRIMP U–Pb zircon ages show that (1) graded volcaniclastic–felsic tuff within the black shale sequence below the banded iron formation in the Cleaverville Formation yields an age of (3114 ±14) Ma; (2) the youngest zircons in sandstones of the Sixty-Six Hill Member, which unconformably overlies pillow basalt of the Regal Formation, yield ages of 3090–3060 Ma; and (3) zircons in sandstones of the Forty-Four Hill Member show two age peaks at 3270 Ga and 3020 Ga. In this way, the Cleaverville Formation was deposited at 3114–3060 Ma and was deformed at 3070–3050 Ma (D_1). Depositional age of the Cleaverville Formation is at least 40–90 Myr older than that proposed in previous studies and pre-dates the Prinsep Orogeny (3070–3050 Ma). After 3020 Ma, D_2 resulted in the formation of a regional strike-slip pull-apart basin in the Cleaverville area. The lower-greenschist-facies volcano-sedimentary rocks are distributed only

within this basin structure. This strike-slip deformation was synchronous with crustal-scale sinistral shear deformation (3000–2930 Ma) in the Pilbara region.

Keywords

banded iron formation, Cleaverville Formation, Cleaverville Syncline, coastal Pilbara Terrane, Mesoarchean, SHRIMP U–Pb zircon age, strike-slip pull-apart basin

1. Introduction

Archean greenstone belts are commonly affected by strike-slip deformation and contain strike-slip pull-apart basins along their structural boundaries (e.g., Kusky & Vearncombe, 1997). This strike-slip deformation in greenstone belts demonstrates the rigidity of the early continental crust. These belts record the final stages of continent formation and stabilization (e.g., Kusky & Vearncombe, 1997). The Pilbara Craton records strike-slip deformation during 2950–2900 Ma in the Kurrana and East Pilbara terranes and the West Pilbara Superterrane (Van Kranendonk, Smithies, Hickman, & Champion, 2007; Hickman, 2012). Examples of this deformation include the Lalla Rookh–Western Shaw structural corridor (Krapez & Barley, 1987; Zegers, de Keijzer, Passchier & White, 1998; Zegers, Wijbrans, & White, 1999; Zegers, Nelson, Wijbrans, & White 2001; Van Kranendonk & Collins, 2001; Van Kranendonk, 2008) and the

Whim Creek and Mallina basins alongside the Sholl Shear Zone (Krapez & Eisenlohr, 1998; Hickman, 2012). The Sholl Shear Zone in the West Pilbara Superterrane bounds the coastal Pilbara and Sholl terranes (Kriewaldt, 1964; Smith et al., 1998; Hickman, 1983, 2001, 2002, 2012). In this paper, we use the term "coastal Pilbara Terrane" for the Karratha and Regal terranes, bounded by the Sholl Shear Zone along its southern boundary (Kiyokawa, Taira, Byrne, Bowring, & Sano, 2002). The Sholl Shear Zone experienced major sinistral tectonism starting at 3020 Ma and was reactivated to produce dextral strike-slip faulting at 2990–2920 Ma (Barley, 1987; Smith et al., 1998; Blewett, 2002; Kiyokawa et al., 2002; Smith, 2003; Hickman, 2012, 2016). The Sholl Shear Zone truncates the coastal Pilbara Terrane and the Whim Creek Group (which formed in a pull-apart or back-arc basin setting) and the Whundo Group in the Sholl Terrane (e.g., Hickman, 2012; Hickman & Van Kranendonk, 2012).

In the coastal Pilbara Terrane, Kiyokawa et al. (2002) described a shallow sedimentary sequence (the Sixty-Six Hill and Forty-Four Hill Members of the Lizard Hills Formation) above a Mesoarchean greenstone sequence (Regal, Dixon Island, and Cleaverville Formations) in the Cleaverville area. Those authors identified three tectonic phases: D_1 folding and thrusting due to collision and accretion of an oceanic island arc and paleo-continent; D_2 left-lateral strike-slip deformation over a wide area;

89 and D_3 dextral strike-slip deformation localized along the Sholl Shear Zone. D_1 and D_2
90 were identified in the greenstone sedimentary and overlying shallow-water sequences in
91 the Cleaverville area.
92 The Cleaverville Formation and its deformation are key to understanding the
93 timing of the island-arc–continent accretion stage. It is important to establish the
94 sedimentary environment, timing, and deformation of the Sixty-Six Hill and Forty-Four
95 Hill Members of the Lizard Hills Formation, as these members represent post-accretion
96 early-stage deformation and the final stabilization of the continental crust. We present
97 new detrital SHRIMP zircon U–Pb ages for three samples, which constrain the
98 sedimentation age of the Cleaverville Formation and the timing of D_1 and D_2
99 deformations of the coastal Pilbara Terrane.

100 ## 2. Geological setting

101 In the coastal Pilbara Terrane, the areas of Cleaverville beach and Dixon Island (Figure
102 1) comprise a greenschist-facies volcaniclastic sequence (the Dixon Island, Cleaverville,
103 and Regal Formations) and a well-preserved quartz-rich sandstone sequence (Lizard
104 Hills Formation; Kiyokawa & Taira, 1998). The low-grade rocks in the Cleaverville
105 area have been examined previously (Ohta, Maruyama, Takahashi, Watanabe, & Kato,
106 1996; Hickman, 1997, 2001, 2002, 2012, 2016; Kiyokawa & Taira, 1998; Kiyokawa et

al., 2002; Van Kranendonk et al., 2007; Shibuya, Kitajima, Komiya, Terabayashi, & Maruyama, 2007). In the Cleaverville area, the volcaniclastic sequence comprises, from bottom to top, the Lagoon Formation (here termed the Lagoon Member), the Lagoon Pillow Basalt (or Regal Formation; Hickman, 2001, 2002), the Dixon Island Formation (Kiyokawa et al., 2006; Kiyokawa, Ito, Ikehara, Yamaguchi, Koge, & Sakamoto, 2012a), the Port Robinson Basalt (Kiyokawa, Koge, Ito, & Ikehara, 2014), and the Cleaverville Formation (Kiyokawa & Taira, 1998; Kiyokawa et al., 2002). The age of the upper Dixon Island Formation has been constrained to 3195 ±12 Ma based on the U–Pb zircon age of a silicic tuff (Kiyokawa et al., 2002).

A fold axis (the Cleaverville Syncline) has been identified in the Cleaverville Formation and Lagoon Pillow Basalt (Kiyokawa & Taira, 1998; Kiyokawa et al., 2002). Two shallow-water sedimentary sequences of the Lizard Hills Formation unconformably overlie the northern part of the Lagoon Member along the Cleaverville Syncline axis and the eastern edge of the Lagoon Pillow Basalt, and are termed the Sixty-Six Hill and Forty-Four Hill Members (Kiyokawa & Taira, 1998; Kiyokawa et al., 2002, 2012a).

Regarding the stratigraphic nomenclature in the Cleaverville area, we mostly follow the maps published by the Geological Survey of Western Australia (e.g.,

Hickman, 2001, 2002, 2016) but use the member names from Kiyokawa and Taira (1998) and Kiyokawa et al. (2012a).

3. Stratigraphy

In this section, we describe the lower-greenschist-facies volcano-sedimentary sequences and the overlying cover sedimentary sequences (Figure 2). This stratigraphy is based mainly on Kiyokawa & Taira (1998), together with our new data.

3.1 Basement greenstone belt

The Regal Formation is divided into the Lagoon Member and Lagoon Pillow Basalt (Kiyokawa & Taira, 1998). To the southeast of the Cleaverville area, the Lagoon Pillow Basalt is overlain by quartz sandstones of the Forty-Four Hill Member, across a marked angular unconformity.

The Dixon Island Formation is exposed mainly on the northern coast of Dixon Island and represents a hydrothermal vent system that formed in a deep oceanic environment (Kiyokawa, Ito, Ikehara, & Kitajima, 2006; Kiyokawa et al., 2012a). The upper part of this formation was drilled by the DXCL Project to collect DX core (Yamaguchi, Kiyokawa, Ito, Ikehara, Kitajima, & Suganuma, 2009; Kiyokawa, Koge, Ito, Ikehara, Kiyajima, Yamaguchi, & Suganuma, 2012b).

142 The Cleaverville Formation is well preserved along the western part (Cleaverville
143 A area) and eastern part (Cleaverville F area) of Cleaverville beach (Figure. 1). The
144 Cleaverville Formation comprises the Black Chert and Banded Iron Formation (BIF)
145 Members.

146 The Black Chert Member is generally poorly exposed and comprises highly
147 weathered white–pink shales and chert-like rocks cropping out along the beach. Using
148 the 1:500 map of the Cleaverville A area compiled by Kiyokawa & Taira (1998), we
149 found well-preserved bedded volcaniclastic–felsic tuff in the upper part of the Black
150 Chert Member (Figure 3a and b). These rocks form 3-m-thick deposits in channels that
151 are a few meters wide. Yellow volcanic and black chert fragments are present within a
152 yellow, fine-grained, silicic volcaniclastic matrix near the base of the bed and fine
153 laminated felsic tuff near the top. In the Cleaverville F area at a site 7 km from the
154 Cleaverville A area, a 50-cm-thick fine-grained felsic tuff is found at the same
155 stratigraphic level. This volcaniclastic–felsic tuff is a key bed and dateable layer in the
156 Black Shale Member. We sampled the yellow, silicic volcaniclastic–felsic tuff at
157 Cleaverville A area for zircon U–Pb dating.

158 The BIF Member comprises well-bedded shale and BIF at topographic highs. The
159 BIF is interbedded with 10-cm-thick shale and chert beds, which thicken gradually to 50

cm over a lateral distance of 50–100 m. The upper part of the BIF Member is separated from the Sixty-Six Hill Member by a fault, which trends east–west through a narrow linear topographic depression (i.e., a fault) in the center of Sixty-Six Hill.

3.2 Cover sequence

3.2.1 Sixty-Six Hill Member

The Sixty-Six Hill Member is found in the core of the Cleaverville Syncline, along the horizontal fold axis, and tightly folded between the Lagoon Pillow Basalt and the BIF Member. The southern boundary might be an unconformable contact with the Lagoon Pillow Basalt, and the northern boundary may be in faulted contact with the BIF Member.

We identified four stratigraphic units: basal, lower, middle, and upper (Figure 2; based on Kiyokawa & Taira, 1998). The basal unit is a poorly sorted, black chert and pebble-rich conglomerate (Figure 3c and d). The lower unit consists of laminated chert, volcaniclastic rock, and pebbly sandstone. The middle unit includes laminated black (Figure 3e) and white–black cherts. The upper unit comprises cross-bedded, coarse-grained, well-sorted, quartz–plagioclase sandstone (Figure 3f) in 20–50-cm-thick beds (Figure 4a and b). The cross-bedding indicates that the younging direction is to the north on the southern limb of the syncline.

3.2.2 Forty-Four Hill Member

The Forty-Four Hill Member is preserved at the eastern boundary of the Lagoon Pillow Basalt and Nicol Well subcomplexes and crops out along two parallel northeast-trending ridges (Forty-Four Hill and Eighty-Seven Hill; Figure 1). In the northwest, this member is composed of well-sorted quartz sandstones. The member contains southeast-dipping beds and overlies the Lagoon Pillow Basalt via an angular unconformity along an erosional contact. This member has been identified as part of the Nickol River Formation (Hickman, 2016). However, based on the stratigraphy, structure, and zircon ages of this member, we identified younger sedimentary sequence than the Nickol River Formation (Kiyokawa & Taira, 1998; Kiyokawa et al., 2002).

There are four main units in the Forty-Four Hill Member (Kiyokawa & Taira, 1998). The basal unit is a 30-m-thick conglomerate containing black quartzite pebbles, which unconformably overlies weathered pillow basalt of the Lagoon Pillow Basalt. The lower unit comprises a cross-bedded sandstone (with herring-bone cross-beds) containing well-rounded quartz grains and black quartz pebbles (Figure 3g). This unit is 100 m thick and forms the northeast-trending ridges of Forty-Four Hill (Figure 1). The middle unit is 120 m thick and comprises poorly sorted, brownish-red, mud-rich sandstones that conformably overlie the lower sandstone units (Figures 3h and 4c), and

196 thin dolomite layers (Kiyokawa & Taira, 1998). This unit is located in a topographic
197 depression along Forty-Four Hill and Eighty-Seven Hill. The upper unit at Eighty-
198 Seven Hill (Figure 1) is folded and comprises an 80-m-thick sequence of bedded white
199 chert, shale, and thin volcanic rocks. The banded white chert is only found in the
200 southeastern part of Eighty-Seven Hill, which is located along the Eighty-Seven Hill
201 Fault (Figure 1).

202 ## 4. Structures

203 A lower-greenschist-facies volcanic–sedimentary sequence crops out in a rhomboidal-
204 shaped area of ~12 km by ~7 km covering Cleaverville beach and Dixon Island (Figure
205 1). This sequence is bounded by upper-greenschist-facies to lower-amphibolite-facies
206 rocks of the Nickol Well and Regal subcomplexes (Kiyokawa et al., 2002). We describe
207 the Cleaverville Syncline and the margins of the rhomboidal-shaped area (northwestern,
208 southern, and southeastern boundaries) in the following sub-sections.

209 ### 4.1 Cleaverville Syncline

210 The Cleaverville Syncline is asymmetrical and it contains the Dixon Island and
211 Cleaverville Formations in the northern limb, and the Lagoon Pillow Basalt in the
212 southern limb. The Sixty-Six Hill Member occurs in the fold core (Kiyokawa & Taira,
213 1998). In the western part of the Sixty-Six Hill area, a tight fold is observed in the

214 Lagoon Pillow Basalt. The eastern part of the fold axis is parallel to an E–W-trending
215 fault. Based on a stratigraphic reconstruction, the total thickness of the Regal, Dixon
216 Island, and Cleaverville Formations is >3–5 km (Kiyokawa & Taira, 1998). However,
217 prior to folding the combined thickness of these formations differed by >800 m in the
218 areas that became the northern and southern limbs of the fold.

219 We propose that the Cleaverville Syncline was formed in four steps (Figure 5),
220 assuming the stratigraphy of this area is consistent spatially (i.e., the Regal, Dixon
221 Island, and Cleaverville Formations from base to top). First, north-verging asymmetric
222 folding occurred after deposition of the Dixon Island and Cleaverville Formations.
223 Second, northward thrusting resulted in the Regal Formation, to the south of the hinge,
224 being moved to a higher stratigraphic position. Along the fold axis, top-to-north
225 thrusting took place and erosion removed >1000 m of the Dixon Island and Cleaverville
226 Formations. The different stratigraphy in the two limbs of the fold might have resulted
227 from top-to-the-north thrusting during the asymmetric folding that formed the
228 Cleaverville Syncline. Third, erosion led to an unconformity between the Sixty-Six Hill
229 Member and Lagoon Pillow Basalt, related to the thrusting and folding (D_1). Finally,
230 further tight folding took place during regional sinistral strike-slip deformation (D_2).
231 Based on the strain ellipsoid of the sinistral deformation, the orientation of the

232 Cleaverville Syncline was also affected by compression during D_2 strike-slip
233 deformation.

234 **4.2 Margins of the rhomboidal-shaped area**

235 **4.2.1 Northwestern boundary**

236 The northwestern boundary of the rhomboidal-shaped area is located offshore from
237 Cleaverville, between the Cleaverville coast and Walcott Island (Figure 1). Walcott
238 Island is <1 km from Cleaverville beach and hosts amphibolite- to upper-greenschist-
239 facies pillow and massive basalts. Metamorphic grade changes markedly along the
240 coast. Sinistral deformation structures (asymmetric faults and shear zones) are observed
241 within the Cleaverville Formation in the Cleaverville A area (Kiyokawa et al., 2002).
242 We identified a SE-dipping, sinistral transtensional fault in the ocean area between
243 Cleaverville beach and Walcott Island (Figure 1; Kiyokawa et al., 2002).

244 **4.2.2 Southern boundary**

245 The southern boundary of the rhomboidal-shaped area, between the Regal Formation
246 (Lagoon Member) and the Karratha Supercomplex, is poorly exposed (Figure 1).
247 Lower-greenschist-facies metavolcanic rocks of the Lagoon Member are in contact with
248 the strongly foliated metasedimentary rocks of the Lydia Mine Complex (Kiyokawa &

Taira, 1998; Figure 1). The contrasting metamorphic grade and foliation trend across the boundary indicate a fault contact.

4.2.3 Southeastern boundary: the strike-slip Eighty-Seven Hill Fault

The linear topography on the southeastern margin of Eighty-Seven Hill, the SE-dipping beds of the Forty-Four Hill Member, and the amphibolite pillow basalt of the Nicol Well complex indicate that a NW-dipping normal fault (the Eighty-Seven Hill Fault; Figure 1) runs along the southeastern side of Eighty-Seven Hill. This fault separates lower-greenschist-facies rocks from lower-amphibolite-facies rocks (Kiyokawa et al., 2002).

A basalt block with pillow lava identical to the Lagoon Pillow Basalt is found in the central-southern area between Forty-Four Hill and Eighty-Seven Hill (Figure 1; Kiyokawa & Taira, 1998). Given the younging direction, this block has been rotated 90° clockwise from the orientation of the Lagoon Pillow Basalt (Kiyokawa & Taira, 1998). The distribution of the SE-dipping sedimentary sequence, the presence of silicified rock along the Eighty-Seven Hill Fault and the occurrence of the rotated block indicate sinistral transtensional deformation.

5. Zircon U–Pb dating

We obtained new zircon U–Pb ages from the Cleaverville Formation and the Lizard Hills Formation. We interpret the ages for the volcaniclastic rocks from the Cleaverville Formation to represent the depositional age. We also obtained an age for detrital zircons from well-sorted sandstones from the upper part of the Sixty-Six Hill Member, and from brownish-red sandstones from the middle part of the Forty-Four Hill Member.

5.1 Analytical methods

Rock samples were cleaned with deionized water in an ultrasonic bath for >5 min, and zircons for U–Pb analysis were separated using magnetic and heavy liquid (1,1,2,2-tetrabromoethane and methylene iodide) techniques at Kyushu University, Japan. Zircons were handpicked to ensure that the selected grains were representative of the zircon population as a whole. Zircon grains were mounted in an epoxy resin disc together with the reference material OG-1 (Stern, Bodorkos, Kamo, Hickman, & Corfu, 2009). The discs were polished to reveal cross-sections through grain centers. Backscattered electron (BSE) and cathodoluminescence (CL) images were obtained using a JEOL JSM-5900LV scanning electron microscope (SEM) with a Gatan mini-CL detector to characterize internal zoning patterns and identify suitable analytical points within each zircon grain. Subsurface mineral inclusions and cracks were identified using

283 an optical microscope with transmitted light. Prior to analysis by a sensitive high-
284 resolution ion microprobe (SHRIMP-II), the surface of the grain mount was washed
285 with dilute HCl and ultrapure water, and then coated with gold.

286 Zircon U–Pb analyses were conducted on the SHRIMP-II housed by the National
287 Institute of Polar Research (NIPR), Tokyo, Japan. An O_2^- primary ion beam of 3.9 nA
288 was used to sputter an analytical spot of 25 μm in diameter on each polished zircon
289 grain. A primary ion beam of 1.1 nA was used for the Cleaverville A area sample, with
290 a spot diameter of 10 μm. We followed the procedure for Pb and U isotopic analyses
291 described by Horie, Takehara, Suda, & Hidaka (2013). We used reference materials
292 FC1 ($^{206}Pb/^{238}U$ age = 1099 Ma; Paces & Miller, 1993) and SL13 (U = 238 ppm;
293 Claoué-Long, Compston, Roberts, & Fanning, 1995) to calibrate the $^{206}Pb/^{238}U$ ratios
294 and U concentrations in zircons, respectively. The OG1 zircon ($^{207}Pb/^{206}Pb$ age = 3465
295 Ma; Stern et al., 2009) was also periodically analyzed with the FC1 zircon to confirm
296 the U/Pb calibration and instrumental mass fractionation of Pb isotopes. U–Pb data were
297 reduced following the method of Williams (1998), using the SQUID2 add-in for the
298 Microsoft Excel macro developed by Ludwig (2009). Common Pb was corrected using
299 the measured ^{204}Pb and the model for common Pb compositions proposed by Stacey and
300 Kramers (1975). The pooled ages presented in this study were calculated after

301 correction for common Pb, using Isoplot/Ex software (Ludwig, 2012). The analytical
302 uncertainties listed in Table 1 and plotted on the concordia diagrams are at the 1σ level
303 and include measurement errors and uncertainties in the common Pb corrections.

304 **5.2 Age of the Black Shale Member of the Cleaverville Formation**

305 We collected graded volcaniclastic–felsic tuff from the middle part of the Black Shale
306 Member of the Cleaverville Formation (Figure 1; Cleaverville A area graded
307 volcaniclastic–felsic tuff; C911 section; sampling location 20°39'51.6"S,
308 116°58'53.4"E). More than 40 kg of sample was collected from the C911 section from
309 which we obtained only 46 zircon grains. The zircons are euhedral or rounded, and fine-
310 grained (> 100 μm); most are pink to clear in color and crack-free. We obtained 46
311 analyses from 43 zircons, and 17 grains had concordant ages. Eleven euhedral zircons
312 yielded a mean age of 3110 Ma, whereas rounded metamict zircons yielded discordant
313 ages between 3700 Ma and 3200 Ma. SEM and optical microscope observations after
314 the SHRIMP analyses indicated Pb loss at spots C91121-02.1 and C91127-03.1 caused
315 by the alteration of zircon (Takehara, Horie, Hokada, & Kiyokawa, 2018).
316 Therefore, we interpret the ages of the youngest nine zircons to represent the age of the
317 graded volcaniclastic–felsic tuff of (3114 ± 14) Ma (Mean sequence weighted deviation:
318 MSWD = 1.6; Figure 6a and b).

5.3 Age of the Sixty-Six Hill Member

We dated the upper part of a well-sorted, medium-grained, quartz–plagioclase arenitic sandstone (sampling location 20°39'38.9"S, 117°00'45.2"E). The samples contain rounded zircon grains that are 100–200 μm long. We collected 89 grains (all concordant) from sample 100912-14 (Figures 3f and 4a) and 106 grains (100 concordant) from sample 100912-15 (Figure 4b). The age results for both samples of detrital zircons fall into two major groups at 3100–3050 and 3300–3200 Ma, along with a minor group at 3700 Ma (Figure 6c and d).

5.4 Age of the Forty-Four Hill Member

We sampled poorly sorted, brownish-red, quartz-rich sandstones with a mud matrix (sampling location 20°41'14.0"S, 117°01'11.5"E) from the middle unit. The zircon grains are rounded and 50–100 μm long. We analyzed 64 spots on 60 zircons from sample 100912-28 (Figures 3h and 4c), and 23 spots yielded concordant ages, with 41 spots being discordant. The zircons from sample 100912-28 cluster into two age groups at 3280–3200 and 3030–3020 Ma (Figure 6c and d).

6. Implications for the timing of sedimentation and tectonism

A D_2 structural map of the coastal Pilbara Terrane is shown in Figure 7. The Cleaverville area contains a clearly defined, rhomboidal-shaped area of lower-

337 greenschist-facies metamorphic rocks. This map also demonstrates that D_1 (i.e.,
338 Cleaverville Syncline formation) and D_2 (i.e., strike-slip deformation) represent distinct
339 deformational stages. The Forty-Four Hill Member was identified along the northeast-
340 trending fault system, parallel to the volcanic rocks of the Fortescue Group. The map
341 also shows the sinistral deformation of the Princep fold axis and western part of the
342 Regal Formation. In addition, most of the lithological subcomplexes that are divided by
343 several mylonitic zones converge into the Sholl Shear Zone (Kiyokawa et al., 2002).
344 Our new age data for the Cleaverville Formation and the Sixty-Six Hill and Forty-
345 Four Hill Members are important for improving our understanding of the depositional
346 age of the Cleaverville Formation, and the timing of collision, continental reworking,
347 and strike-slip pull-apart basin formation associated with D_2 strike-slip faulting. We are
348 able to constrain the sedimentation and deformation history in the Cleaverville area
349 using our new age data, integrated with previous studies of sedimentation in the central
350 and eastern Pilbara (Figure 8). These data constrain the D_1 to D_2 deformation phases of
351 Kiyokawa et al. (2002) and enable us to present a detailed history of the sedimentation
352 and tectonic development.

6.1 Depositional age of the Cleaverville Formation

The depositional age of the lower part of the Dixon Island Formation is (3195 ±12) Ma (Kiyokawa et al., 2002), and the new age of the upper part of the Black Shale Member is (3114 ±14) Ma, which represents the maximum depositional age. Both ages were determined on samples from thin volcanic and tuff beds.

Nelson (1998) reported zircon ages of 3022 Ma and 3060 Ma for volcaniclastic rocks described as being part of the Cleaverville Formation (sample number 127330; sampling location 20°39'34"S, 117°01'20"E; Figure 1). This sample location, now identified as from the lower unit of the Sixty-Six Hill Member, and the age accuracy is not well constrained. Our sandstone age data from the upper part of the Sixty-Six Hill Member are dominated by 3060 Ma detrital grains. As such, the uppermost Cleaverville Formation must be older than 3060 Ma. Detrital zircon grains with ages of 3090–3060 Ma in the Sixty-Six Hill Member might be related to the initial stage of Cleaverville Syncline formation after deposition of the Cleaverville Formation. Deposition of volcaniclastic rocks within the Sixty-Six Hill Member and Cleaverville Syncline deformation were related to D_1 island arc accretion.

Therefore, we consider that sedimentation of the Cleaverville Formation started at 3120 Ma and ended prior to 3090–3060 Ma. This formation was then continuously

371 deformed during 3060–3020 Ma, coeval with the Prinsep Orogeny. The new age is 40–
372 80 Myr older than previous estimates of the sedimentation age (Smithies & Farrell,
373 2000; Blewett, 2002; Hickman, 2016) of the BIF of the Cleaverville Formation.

374 In addition, the 3105 Ma depositional age for the Nimingarra Iron Formation in
375 the Shay Gap belt from the East Pilbara Terrane (Sheppard, Krapez, Zi, Rasmussen, &
376 Fletcher, 2017) is similar to our age for the Cleaverville Formation. However, the 3105
377 Ma age of the Nimingarra Iron Formation is uncertain because the youngest zircon was
378 dated at 3027 Ma, and the spread of zircon ages used in the calculation was 120 Myr.

379 Despite the uncertainties, the 3110–3060 Ma sedimentation age is important for
380 constraining the accretion and amalgamation of the coastal Pilbara Craton. It is apparent
381 that a BIF was deposited over a more regionally extensive area than previously thought.

382 **6.2 Characteristics of the strike-slip pull-apart basin**

383 The rocks of the Regal, Dixon Island, and Cleaverville Formations have been affected
384 by prehnite–pumpellyite–lower-greenschist-facies metamorphism. At these grades, the
385 rocks experienced temperatures of 250–350 °C and pressures of 2–7 kbar (Kiyokawa et
386 al., 2002). Beyond the outcrops of the Cleaverville low-grade rocks, the rocks are upper
387 greenschist–lower amphibolite-facies, indicating temperatures of 400–550 °C and
388 pressures of 3–10 kbar. This shows that the Cleaverville low-grade rocks experienced

389 temperatures 150–200 °C lower than those of the surrounding rocks. If the geothermal
390 gradient was double the modern value (2–4 × 10^{-2} °C/m; Martin, 1986), then this
391 suggests that the strike-slip pull-apart basin generated 2000–4000 m of vertical offset.
392 Most of the sediments containing clastic rocks of continental origin are now only
393 preserved in the Forty-Four Hill Member along the fault due to erosion, which has
394 exposed the basement greenstone sequence. This pull-apart transtensional system might
395 explain why low-grade greenstone sequences are preserved and unconformable quartz-
396 rich sedimentary sequences are present in the Cleaverville area.

397 **6.3 Strike-slip pull-apart basin formation**

398 There are two age groups of detrital zircons (3270 Ma and 3020 Ma) in the Forty-Four
399 Hill Member. However, the Sixty-Six Hill Member does not contain the 3270 Ma and
400 3020 Ma age groups. We interpret that the older zircon age group from the Forty-Four
401 Hill Member (3300–3270 Ma) was sourced from the Karratha Granitoid and that the
402 younger group of zircons (3020 Ma) was derived from southern granitoids (e.g.,
403 Harding subcomplex: Kiyokawa et al., 2002; Orpheus Supersuite monzogranite:
404 Hickman & Van Kranendonk, 2012) and from quartz porphyry intrusions in the Nickol
405 Well subcomplex (Kiyokawa et al., 2002). Therefore, these 3020 and 3270 Ma granitic
406 rocks must have been subaerially exposed near the Forty-Four Hill Member at the time

407 of deposition. During the sedimentation of the Sixty-Six Hill Member, these rocks were
408 not exposed at the surface. In addition, Nelson (1997) reported an age of (3015 ± 5) Ma
409 for strongly foliated volcaniclastic–sedimentary rocks (some ages of 3270–3250 Ma)
410 from near Wickham (sample number 136899; 20°41'17"S, 117°05'07"E). This sample
411 was collected from between chert and iron formation sequences, and we consider it to
412 be correlative with the Forty-Four Hill Member.

413 The strong D_2 sinistral shear fabric in the entire coastal Pilbara Terrane was
414 related to movement of the Sholl Shear Zone (e.g., Sun & Hickman, 1998; Kiyokawa et
415 al., 2002; Hickman, 2004; Hickman, Huston, Van Kranendonk, & Smithies, 2006). We
416 propose that there were two stages of movement on the Sholl Shear Zone. (1) Stage 1:
417 sinistral movement of up to 200 km that formed the Whim Creek Basin. Previous
418 studies have identified an earlier stage of movement up to 200 Myr before deposition of
419 the Whim Creek Group (Hickman, 2016). (2) Stage 2: late-stage dextral movement at
420 2920 Ma, which involved <50 km of movement (Sun & Hickman, 1998). The Karratha
421 Granitoid (Prinsep Dome) might have been elongated by the D_2 sinistral deformation.

422 Around this time, several strike-slip pull-apart basins formed throughout the
423 Pilbara Craton (e.g., Krapez & Barley, 1987; Krapez & Eisenlohr, 1998; Van
424 Kranendonk & Collins, 1998). The Lalla Rookh–Western Shaw structural corridor is a

425 >150-km-long intracrustal deformation zone in eastern Pilbara, which was deformed by
426 sinistral strike-slip deformation at 2930 Ma (Van Kranendonk, 2008). The Sholl Shear
427 Zone also experienced significant movement from 3070 Ma to 2920 Ma (Smith et al.,
428 1998; Hickman, 2004). As such, the Pilbara Craton was affected by region-wide,
429 sinistral strike-slip deformation and the "Cleaverville pull-apart basins" might have
430 formed at this time.

431 The formation of the coastal Pilbara Terrane occurred as follows: (1) onset of
432 deposition and formation of an oceanic island arc at 3200–3060 Ma; (2) arc–continent
433 accretion at 3070–3050 Ma; (3) strike-slip faulting and strike-slip pull-apart basin
434 formation during continent stabilization at 3000–2930 Ma; and (4) rigid craton
435 formation at 2930–2800 Ma. It took 100–180 Myr to add this new continental crust to
436 the Pilbara Craton.

437 ## 7. Conclusions

438 A detailed geological and zircon dating study of the Cleaverville Formation allows the
439 sedimentation and tectonic history of these rocks to be divided into the following three
440 stages.

441 1) Formation of the volcanic–sedimentary sequence (Dixon Island and
442 Cleaverville Formations) at ca. 3200–3060 Ma. In particular, the BIF Member of the

443 Cleaverville Formation was deposited from 3114 Ma to 3060 Ma. This depositional age
444 is 40–90 Myr older than that proposed in previous studies and pre-dates the Prinsep
445 Orogeny (3070–3050 Ma). The Cleaverville Formation contains a key banded iron
446 formation, which allows stratigraphic correlation from east to west across the
447 Mesoarchean Pilbara Supergroup. The age of the Cleaverville Formation (3.1 Ga) has
448 implications for previous interpretations of stratigraphy in Pilbara.

449 2) Sedimentation of the Sixty-Six Hill Member, which is in unconformable
450 contact with the Lagoon Pillow Basalt and in fault contact with the Cleaverville
451 Formation. Sedimentation was associated with the formation of the Cleaverville Syncline.
452 This deformation is identified as phase D_1 (accretion and collision), which occurred at
453 3070–3050 Ma. This deformation was thus associated with the regional collision event of
454 the Prinsep Orogeny. At this time, the coastal Pilbara Terrane collided with and began to
455 cratonize the Central Pilbara.

456 3) NE-trending strike-slip faults bounding a strike-slip pull-apart basin created a
457 tidal, shallow-ocean depositional setting above the greenstone section after D_1
458 deformation. The strike-slip faults might have had vertical offsets of 2000–4000 m and
459 most of these sedimentary rocks are now eroded. Sandstones with detrital zircon ages of
460 3020 Ma (similar to the Orpheus Supersuite of the Harding complex; Hickman and Van

461 Kranendonk, 2012) and 3270 Ma (similar to the Karratha Granitoid) in this basin indicate
462 that exhumation and erosion occurred prior to strike-slip deformation in the coastal
463 Pilbara Terrane. We propose that this local strike-slip pull-apart basin system was related
464 to the D_2 deformation that affected the entire Pilbara Craton and generated left-lateral
465 shear related to the Sholl Shear Zone from 3000 Ma to 2930 Ma. This strike-slip
466 deformation was the final cratonization event of the Pilbara Craton and occurred 70–140
467 Myr after the Prinsep Orogeny.

Acknowledgments

We acknowledge fruitful discussions with Minoru Ikehara, and Kosei Yamaguchi about our research. Kim North, and Kiyoshi Takeda assisted with fieldwork in the Pilbara area. We thank Arthur Hickman and an anonymous reviewer for their detailed reviews of an earlier version of this paper. This study was supported by Grants-in-Aid from the Japanese Ministry of Education, Culture, Sports, Science, and Technology (KAKENHI 22253008 and 26257211). We acknowledge the assistance of the 2013 to 2017 short-term research programs of Kyushu University and the Kochi Core Center. This study was undertaken with the cooperation of the Center for Advanced Marine Core Research (CMCR) of Kochi University (Grants 13A002, 13B002, 14A009, 14B007, 15A050, 15A045, 16A038, 16B034, 17A002, and 17B002).

480 **References**

481 Barley M. E. (1987). The Archean Whim Creek Belt: an ensialic fault-bounded basin in
482 the Pilbara Block, Australia. *Precambrian Research*, *37*, 199–215.

483 Black L. P., Kamo S. L., Allen C. M., Davis D. W., Aleinikoff J. N., Valley J. W.,
484 Mundil R., Campbell I. H., Korsch R. J., Williams I. S., & Foudoulis C. (2004).
485 Improved $^{206}Pb/^{238}U$ microprobe geochronology by the monitoring of a trace-
486 element-related matrix effect; SHRIMP, ID–TIMS, ELA–ICP–MS and oxygen
487 isotope documentation for a series of zircon standards. *Chemical Geology*, *205*, 115–
488 140.

489 Blewett R. S. (2002). Archean tectonic processes: a case for horizontal shortening in the
490 North Pilbara Granite–Greenstone Terrane, Western Australia. *Precambrian*
491 *Research*, *113*, 87–120.

492 Claoué-Long J. C., Compston W., Roberts J., & Fanning C. M. (1995). Two
493 Carboniferous ages: a comparison of SHRIMP zircon dating with conventional
494 zircon ages and $^{40}Ar/^{39}Ar$ analysis. In: Berggren W. A., Kent D. V., Aubrey M. P., &
495 Hardenbol J. (Eds.), Geochronology Time Scales and Global Stratigraphic
496 Correlation. *Society for Sedimentary Geology Special Publication*, *54*. 3–21.

Hickman A. H. (1997). A revision of the stratigraphy of Archaean greenstone successions in the Roebourne–Whundo area, west Pilbara. (Annual Review 1996–97, pp.76–82) Geological Survey of Western Australia.

Hickman A.H. (2001). *Geology of the Dampier 1:100 000 sheet.* (1:100 000 Geological Series Explanatory Notes, 39 pp.), Geological Survey of Western Australia.

Hickman A. H. (2002), *Geology of the Roebourne 1:100 000 sheet.* (1:100 000 Geological Series Explanatory Notes, 35 pp.), Geological Survey of Western Australia.

Hickman A. H. (2004), Two contrasting granite–greenstones terranes in the Pilbara Craton, Australia: evidence for vertical and horizontal tectonic regimes prior to 2900 Ma. *Precambrian Research*, *131*, 153–172.

Hickman A. H. (2012). Review of the Pilbara Craton and Fortescue Basin, Western Australia: crustal evolution providing environments for early life. *Island Arc*, *21*, 1–31.

Hickman A. H. (2016). Northwest Pilbara Craton: A Record of 450 million years in the growth of Archean continental crust. (Report 160, 104 pp.), Geological Survey of Western Australia.

514 Hickman A. H., Huston D. L., Van Kranendonk M. J., & Smithies R. H. (2006).
515 *Geology and mineralization of the west Pilbara — a field guide*, (Record 2006/17, 50
516 pp.), Geological Survey of Western Australia.
517 Hickman A. H., & Van Kranendonk M. J. (2012). Early Earth evolution: evidence from
518 the 3.5–1.8 Ga geological history of the Pilbara region of Western Australia.
519 *Episodes*, *35*(1), 283–297.
520 Horie K., Takehara M., Suda Y., & Hidaka H. (2013). Potential Mesozoic reference
521 zircon from Unazuki plutonic complex: geochronological and geochemical
522 characterization. *Island Arc*, *22*, 292–305.
523 Kiyokawa S., Ito T., Ikehara M., & Kitajima F. (2006). Middle Archean volcano-
524 hydrothermal sequence: bacterial microfossil-bearing 3.2-Ga Dixon Island
525 Formation, coastal Pilbara Terrane, Australia. *Geological Society of America*
526 *Bulletin, 118*, 3–22.
527 Kiyokawa S., Ito T., Ikehara M., Yamaguchi K.E., Koge S., & Sakamoto R. (2012a).
528 Lateral variations in the lithology and organic chemistry of a black shale sequence on
529 the Mesoarchean sea floor affected by hydrothermal processes: the Dixon Island
530 Formation of the coastal Pilbara Terrane, Western Australia. *Island Arc*, *21*, 66–78.

Kiyokawa S., Koge S., Ito T., & Ikehara M. (2014). An ocean-floor carbonaceous sedimentary sequence in the 3.2-Ga Dixon Island Formation, coastal Pilbara terrane, Western Australia. *Precambrian Research*, *255*, 124–143.

Kiyokawa S., Koge S., Ito T., Ikehara M., Kiyajima F., Yamaguchi K.E., & Suganuma, Y. (2012b). *Preliminary report on the Dixon Island–Cleaverville Drilling Project, Pilbara Craton, Western Australia*. (Record 2012/14, 39 pp.), Geological Survey of Western Australia.

Kiyokawa S., & Taira A. (1998). The Cleaverville Group in the West Pilbara coastal granitoid–greenstone Terrane of Western Australia: an example of a Mid-Archaean immature oceanic island-arc succession. *Precambrian Research*, *88*, 109–142.

Kiyokawa S., Taira A., Byrne T., Bowring S., & Sano Y. (2002). Structural evolution of the middle Archean coastal Pilbara Terrane, Western Australia. *Tectonics, 21*, 1–24.

Krapez B., & Barley M. E. (1987). Archean strike-slip faulting and related ensialic basins evidence from the Pilbara Block, Australia. *Geological Magazine*, *124*, 555–567.

Krapez B., & Eisenlohr B. (1998). Tectonic settings of Archean (3325–2775 Ma) crustal–supracrustal belts in the West Pilbara Block. *Precambrian Research*, *88*, 173–205.

549 Kriewaldt M. J. B. (1964). *Dampier and Barrow Island W.A.,* (1,250,000 Geological
550 Series, Explanatory Notes SF/50-2 and SF/50-1, 13 pp.), Geological Survey of
551 Western Australia.
552 Kusky T. M., & Vearncombe J. R. (1997). Structural Aspects. In: M. de Wit., & Ashwal
553 L. (Eds.), *Greenstone Belts* (pp. 91–124), New York, Oxford Univ. Press.
554 Ludwig K. R. (2009). SQUID 2: a user's manual, Berkeley Geochronology Center
555 Special Publication, Berkeley, 2, 104 pp.
556 Ludwig K. R. (2012). Isoplot 3.75-4.15: a geochronological toolkit for Microsoft Excel,
557 Berkeley Geochronology Center Special Publication, Berkeley, California.
558 Martin H. (1986). Effect of steeper Archean geothermal gradient on geochemistry of
559 subduction-zone magmas. *Geology*, 14, 9, 753-756.
560 Nelson D. R. (1997). *Compilation of SHRIMP U–Pb zircon geochronology data, 1996*,
561 (Record 1997/2, 242 pp.), Geological Survey of Western Australia.
562 Nelson D. R. (1998). *Compilation of SHRIMP U–Pb zircon geochronology data, 1997*,
563 (Record 1998/2, 222 pp.), Geological Survey of Western Australia.
564 Ohta H., Maruyama S., Takahashi E., Watanabe Y., & Kato Y. (1996). Field
565 occurrence, geochemistry and petrogenesis of the Archaean Mid-Oceanic Ridge

566 Basalts (AMORBs) of the Cleaverville area, Pilbara Craton, Western Australia:
567 *Lithos*, *37*, 199–221.
568 Paces J. B., & Miller J. D. (1993). Precise U–Pb ages of Duluth Complex and related
569 mafic intrusions, northeastern Minnesota: Geochronological insights to physical,
570 petrogenetic, paleomagnetic, and tectonomagmatic processes associated with the 1.1
571 Ga Midcontinent Rift System. *Journal of Geophysical Research*, *98*, 13997–14013.
572 Sheppard S., Krapez B., Zi J. W., Rasmussen B., & Fletcher I. (2017). SHRIMP U–Pb
573 zircon geochronology establishes that banded iron formations are not
574 chronostratigraphic markers across Archean greenstone belts. *Precambrian*
575 *Research*, *292*, 290–304.
576 Shibuya T., Kitajima K., Komiya T., Terabayashi M., & Maruyama S. (2007). Middle
577 Archean ocean ridge hydrothermal metamorphism and alteration recorded in the
578 Cleaverville area, Pilbara Craton, Western Australia: *Journal of Metamorphic*
579 *Geology*, *25*, 751–767.
580 Smith J. B. (2003). The episodic development of intermediate to silicic volcano-
581 plutonic suites in the Archean West Pilbara, Australia. *Chemical Geology*, *194*, 275–
582 295.

583 Smith J. B., Barley M. E., Groves D. I., Krapez B., McNaughton N. J., Bickle M. J., &
584 Chapman H. J. (1998). The Sholl Shear Zone, West Pilbara: Evidence for a domain
585 boundary structure from integrated tectonic analysis, SHRIMP U–Pb dating, isotopic
586 and geochemical data of granitoids, *Precambrian Research*, *88*, 143 – 171.
587 Smithies R. H., & Farrell T. (2000). *Geology of the Satirist 1:100 000 sheet* (1:100 000
588 Geological Series Explanatory Notes, 42 pp.), Geological Survey of Western
589 Australia.
590 Stacey J. S., & Kramers J. D. (1975). Approximation of terrestrial lead isotope
591 evolution by a two-stage model. *Earth and Planetary Science Letters*, *26*, 207–221.
592 Stern R. A., Bodorkos S., Kamo S. L., Hickman A. H., & Corfu F. (2009).
593 Measurement of SIMS instrumental mass fractionation of Pb-isotopes during zircon
594 dating. *Geostandards and Geoanalytical Research*, *33*, 145–168.
595 Sun S.S, & Hickman A.H. (1998). New Nd-isotopic and geochemical data from the
596 west Pilbara—implications for Archaean crustal accretion and shear zone
597 development. Research Newsletter, no. 28, pp. 25–29, Australian Geological Survey
598 Organisation.
599 Takehara M., Horie K., Hokada T., & Kiyokawa S. (2018). New insight into
600 disturbance of U–Pb and trace-element systems in hydrothermally altered zircon via

SHRIMP analyses of zircon from the Duluth Gabbro. *Chemical Geology*, *484*, 168–178.

Van Kranendonk M.J. (2008). Structural geology of the central part of the Western Shaw – Lalla Rookh structural corridor, Pilbara Craton, Western Australia. (Report No. 103, 29 pp). Geological Survey of Western Australia.

Van Kranendonk M.J., & Collins W.J. (1998). The tectonic and metal orogenic evolution of the Pilbara Craton: timing and tectonic significance of Late Archean, sinistral strike-slip deformation in the Central Pilbara Structural Corridor, Pilbara Craton, Western Australia. *Precambrian Research*, *88*, 207–232.

Van Kranendonk M.J., Smithies R.H., Hickman A.H., & Champion D.C. (2007). Secular tectonic evolution of Archaean continental crust: interplay between horizontal and vertical processes in the formation of the Pilbara Craton, Australia. *Terra Nova*, *19*(1), 1–38.

Watt J. H. (1995). *West Pilbara: Total Magnetic Intensity Map Preliminary Edition*. Department of Minerals and Energy Western Australia. NGMA and AGSO.

Williams I. S. (1998). U–Th–Pb geochronology by ion microprobe. In: McKibben M. A., Shanks III W. C., & Ridley W. I. (Eds.), Applications of Microanalytical

Techniques to Understanding Mineralizing Processes. *Reviews in Economic Geology*, *7*, 1–35.

Yamaguchi K., Kiyokawa S., Ito T., Ikehara M., Kitajima F., & Suganuma Y. (2009). Clues of Early life: Dixon Island – Cleaverville Drilling Project (DXCL-dp) in the Pilbara Craton of Western Australia. *Scientific Drilling*, *7*, 34–37.

Zegers T. E., de Keijzer M., Passchier C. W., & White S. H. (1998). The Mulganfinnaha shear zone; and Archean crustal-scale strike-slip zone, eastern Pilbara, Western Australia. *Precambrian Research*, *88*, 233–248.

Zegers T. E., Nelson D. R., Wijbrans J. R. C., & White S. H. (2001). SHRIMP U–Pb zircon dating of Archean core complex formation and pancratonic strike-slip deformation in the East Pilbara Granite–Greenstone Terrane. *Tectonics*, *20*(6), 883–908.

Zegers T. E., Wijbrans J. R., & White S. H. (1999). $^{40}Ar/^{39}Ar$ age constraints on tectonothermal events in the Shaw area of the eastern Pilbara granite–greenstone Terrane (W Australia): 700 Ma of Archean tectonic evolution. *Earth and Planetary Science Letters*, *311*, 45–81.

Figure and Table Captions

Figure 1. Geological map of the study area. (a) Location map of the Pilbara Craton. (b) Geological map of the Cleaverville area, coastal Pilbara Terrane (after Kiyokawa & Taira, 1998; Kiyokawa et al., 2006, 2012a). Red stars show the sample locations of new zircon U–Pb ages from this study. CL A is the Cleaverville A area, and CL F is the Cleaverville F area.

Figure 2. Stratigraphic columns of the Dixon Island, Cleaverville, and Lizard Hills Formations (after Kiyokawa & Taira, 1998; Kiyokawa et al., 2012a). Stars indicate samples collected for age dating. The numbers of the stars correspond to the numbers on the geological map (Figure 1). Red stars represent samples of this study.

Figure 3. Outcrop photographs of the Cleaverville area. (a) Overview of zircon U–Pb age data for the silicic volcaniclastic–felsic tuff section of the Black Chert Member in the Cleaverville Formation. The silicic volcaniclastic–felsic tuff bed is 2.5 m thick and occurs in a 7-m-wide channelized depression. The lower part of the bed contains black chert fragments, and the upper part contains finely laminated tuff and grades into a black chert sequence. (b) Close-up of the silicic volcaniclastic–felsic tuff in (a). Zircon grains were extracted from 40 kg samples of fine-grained yellow silicic tuff (matrix of black chert fragments). (c) Black chert and pebble-rich conglomerate in the lower part

653 of the Sixty-Six Hill Member. (d) Close-up of the granule-sized chert–volcaniclastic
654 rocks in the middle part of the Sixty-Six Hill Member. (e) Bedded black cherts from the
655 middle part of the Sixty-Six Hill Member. (f) Homogeneous, fine- to medium-grained,
656 gray sandstone (wacke) in the upper part of the Sixty-Six Hill Member. Sample 100912-
657 15 was taken from these rocks (Figure 4b). (g) Well-sorted, coarse-grained sandstone
658 from the lower part of the Forty-Four Hill Member, with well-preserved herring-bone
659 cross-stratification. The sandstone channel beds are filled with black chert conglomerate
660 and unconformably overlie the Lagoon Pillow Basalt (Regal Formation). (h) Poorly
661 sorted, pebbly, coarse-grained, red sandstone from the middle part of the Forty-Four
662 Hill Member. Pebbles of white vein quartz and sandstone are found in this unit.

663 Figure 4. Thin section photomicrographs of dated sandstone samples from the
664 Lizard Hills Formation (left-hand side = plane-polarized light; right-hand side = cross-
665 polarized light). a1: Sample 100912-14 (plane-polarized light). Homogeneous, fine- to
666 medium-grained sandstone from the upper part of the Sixty-Six Hill Member,
667 containing rounded grains of quartz, chert, and plagioclase (Figure. 3f). Each grain is
668 coated by silica. a2: Sample 100912-14 in cross-polarized light. b1: Sample 100912-15
669 (plane-polarized light). Homogeneous, medium-grained sandstone from the upper part
670 of the Sixty-Six Hill Member, containing rounded grains of quartz, chert, and

671 plagioclase, and white mica in the matrix. b2: Sample 100912-15 (cross-polarized
672 light). c1: Sample 100912-28c-50 (plane-polarized light). Poorly sorted red sandstone
673 from the middle of the Forty-Four Hill Member. c2: Sample 100912-28c-50 (cross-
674 polarized light).

675 Figure 5. Schematic model of the formation of the Cleaverville Syncline and
676 sedimentation of the Sixty-Six Hill Member. The top figure shows the original
677 stratigraphy. The south limb (Lagoon Pillow Basalt) was folded and thrusted during the
678 early stage of fold development. The fold axis area was the site of sedimentation of the
679 Sixty-Six Hill Member after thrusting. After sedimentation of the Sixty-Six Hill
680 Member, compression continued and a tight fold formed during D_2 deformation.

681 Figure 6. Detrital zircon U–Pb age data. (a) Wasserburg concordia plot for zircons
682 from the fine-grained matrix of the volcaniclastic rocks (fine-grained silicic tuff matrix
683 containing black chert pebbles) in the Black Shale Member of the Cleaverville
684 Formation (sample C911: Location 3 in Figure 1). (b) Backscattered electron images of
685 zircon grains from sample C911. Red circles indicate sites that were dated. (c)
686 Wasserburg concordia plot for zircons in sandstones from the Sixty-Six Hill Member
687 (samples 100912-14 and 100912-15: Locations 4 and 5 in Figure 1) and the Forty-Four

688 Hill Member (sample 100912-28: Location 6 in Figure 1). (d) Age histograms of the

689 zircon ages from (c).

690 Figure 7. D_2 structural map of the coastal Pilbara Terrane. The estimate of ocean

691 area is based on aeromagnetic images from GSWA (Watt, 1995).

692 Figure 8. Schematic geological history of the Cleaverville area of the coastal

693 Pilbara Terrane.

694 Table 1. U–Pb age data for felsic tuff and sandstone detrital zircons.

Figure 1 ① Kiyokawa et al. (2002), ② Nelson (1998), ③—⑥ This study

Figure 2

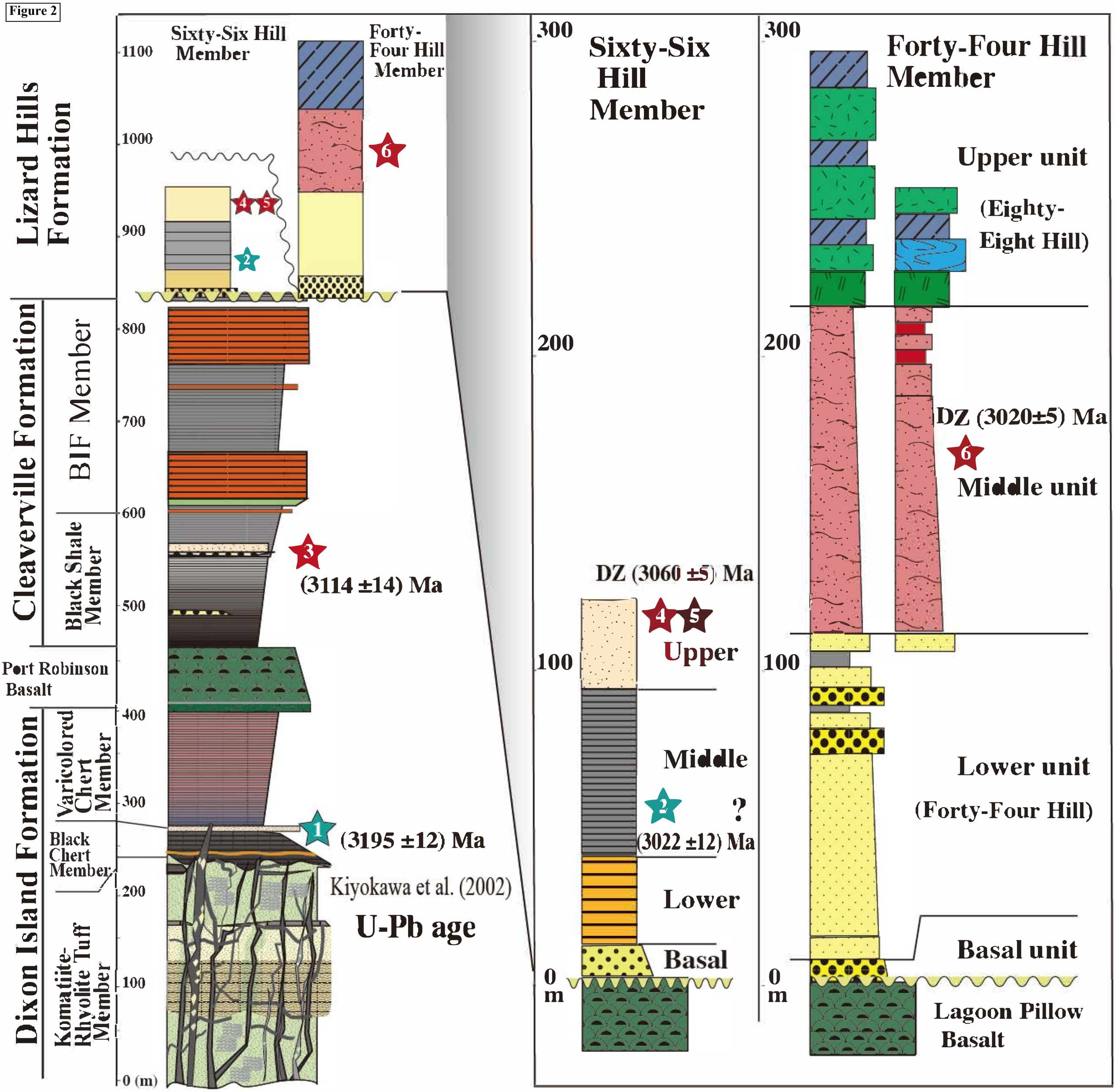

LEGEND

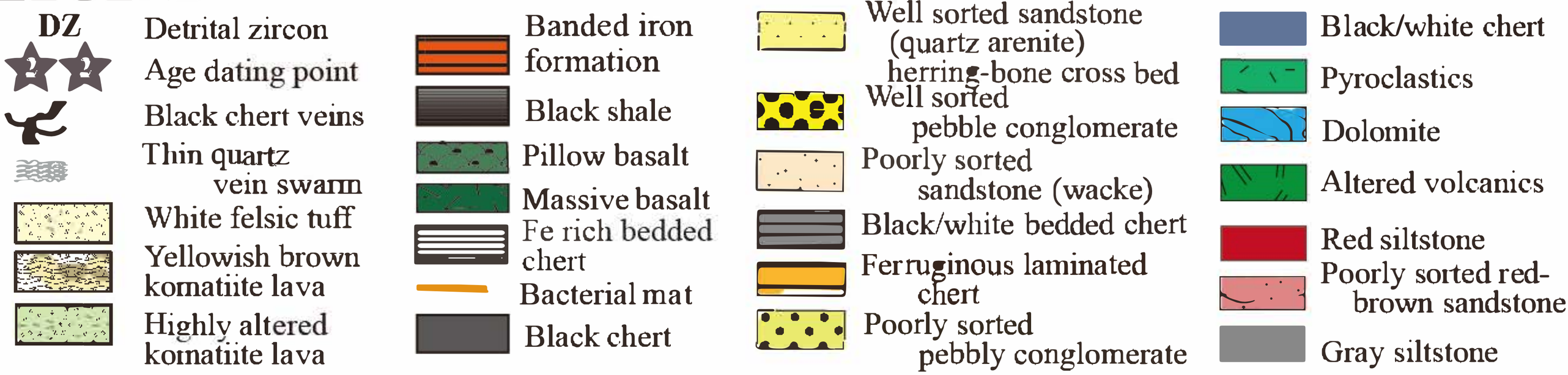

Figure 3


a
upper
lower


b
bedding
upper
Lower


c


d
Nikon


e
BEAR & JACKSON


f


g


h
Nikon

Figure 4

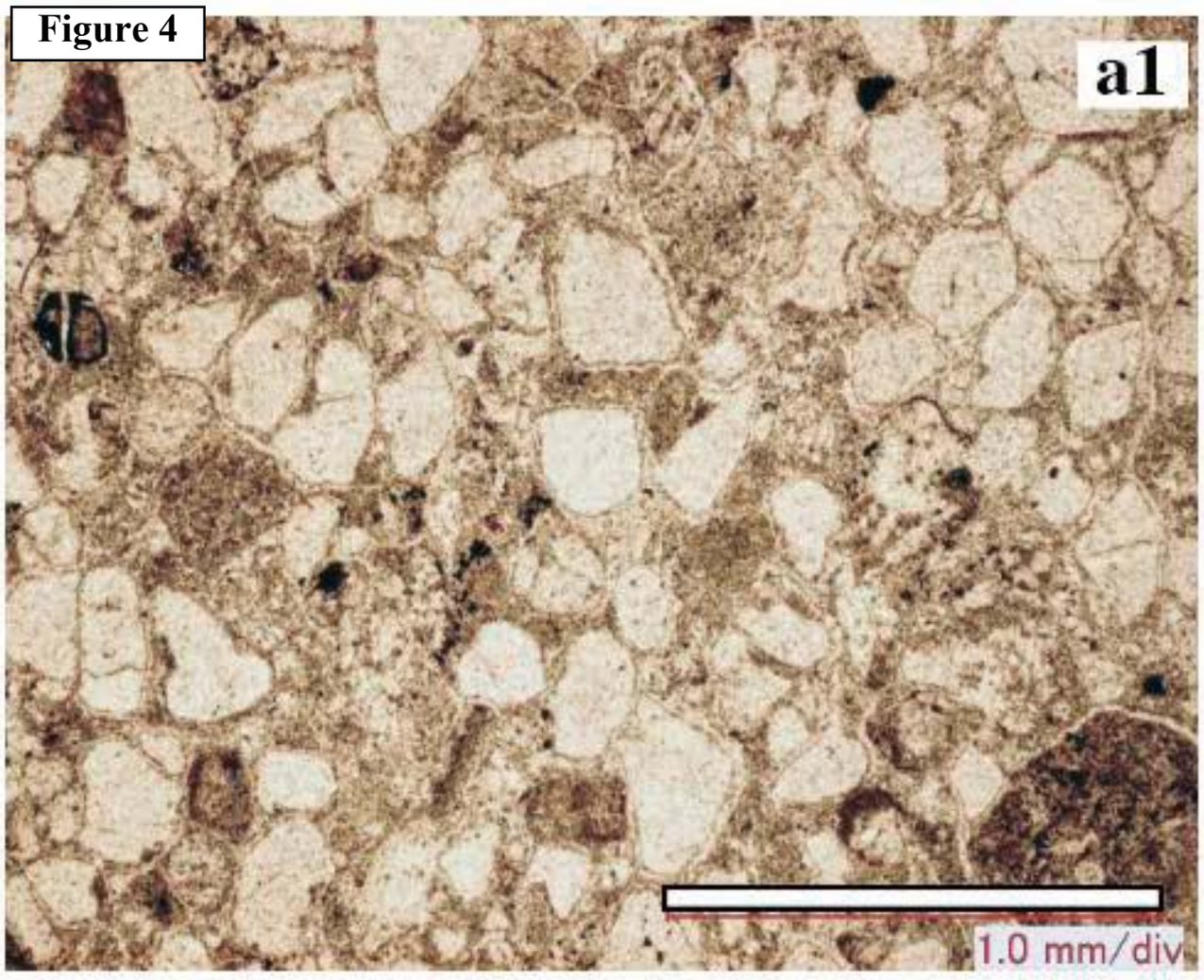
a1
1.0 mm/div

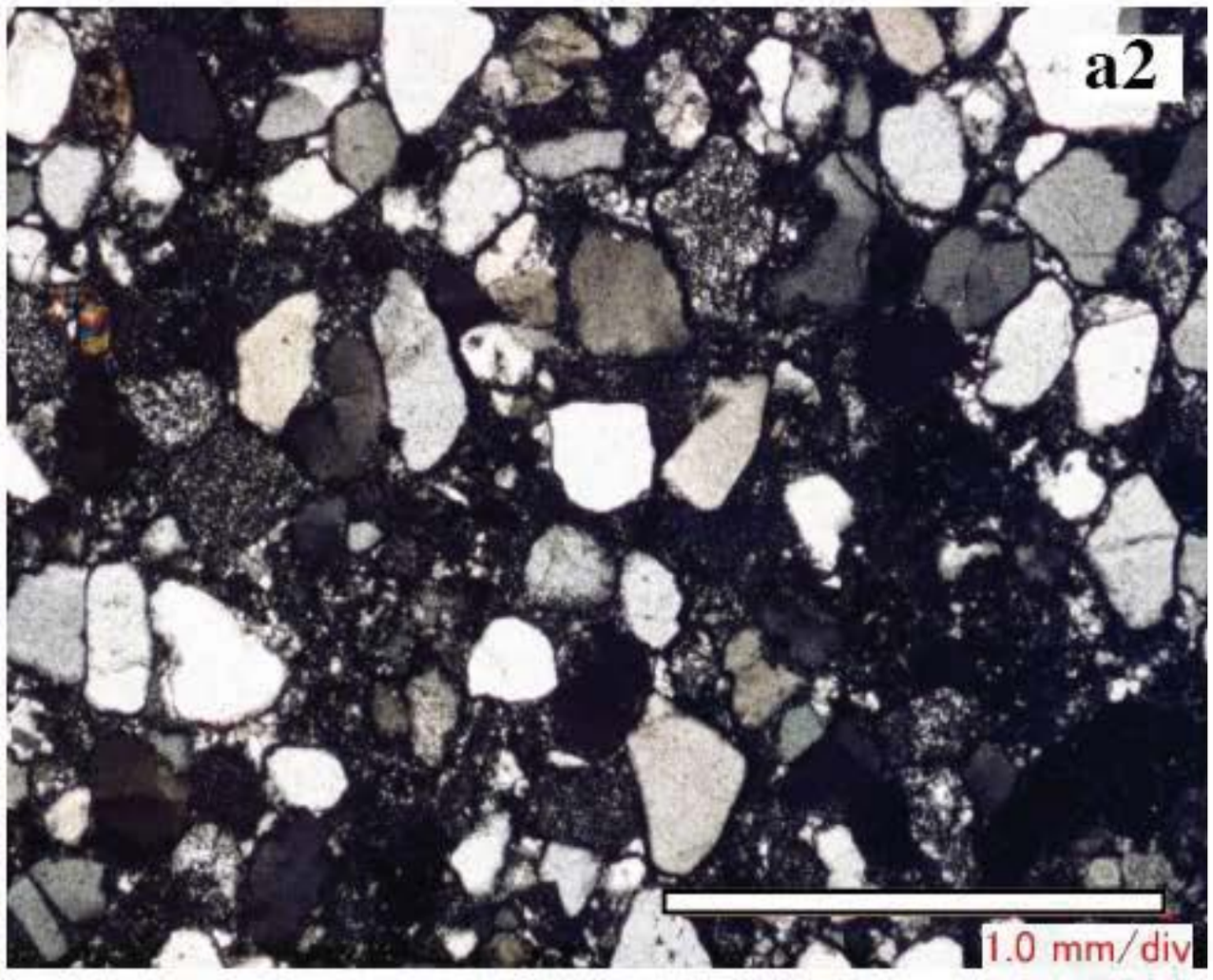
a2
1.0 mm/div

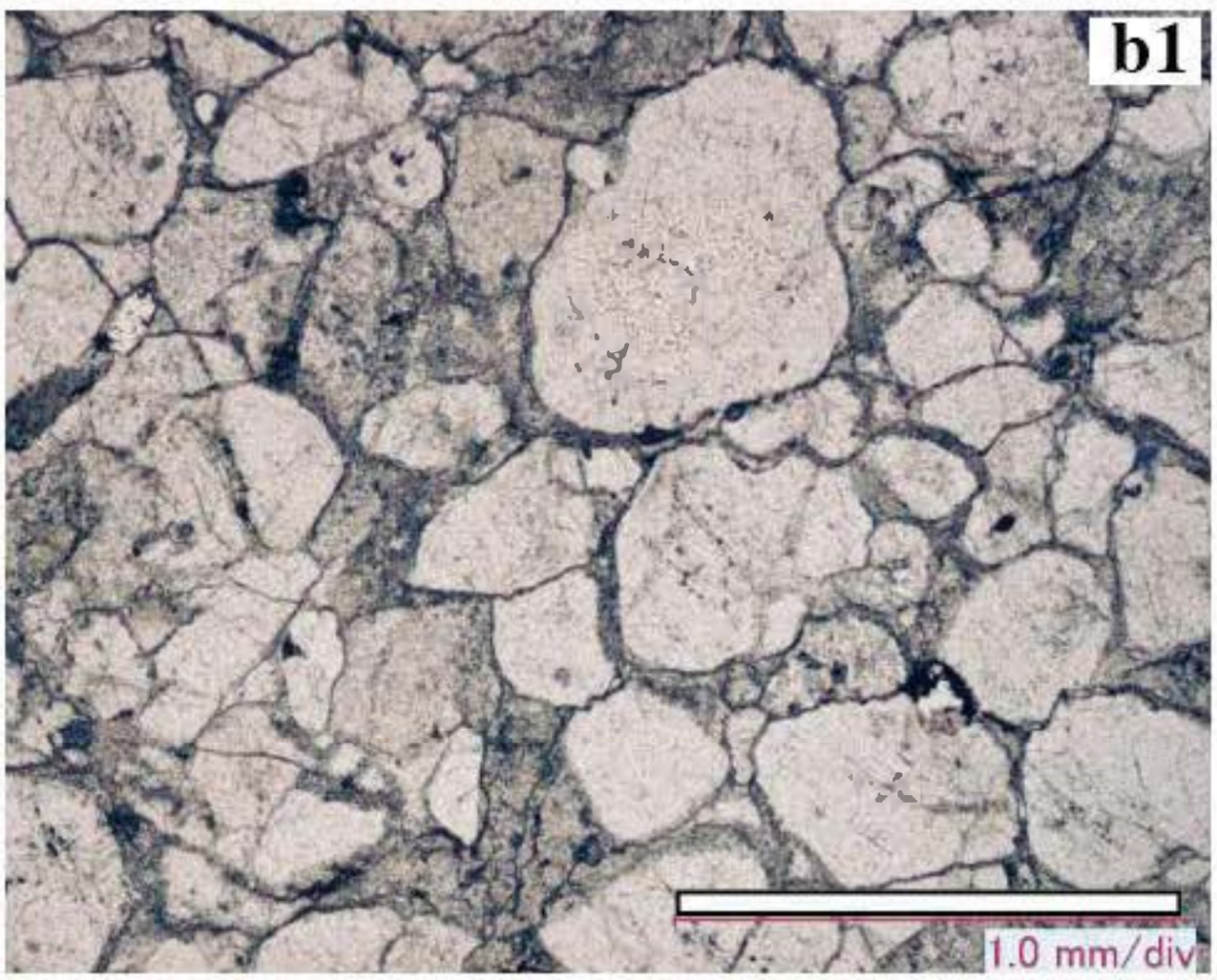
b1
1.0 mm/div


b2
1.0 mm/div

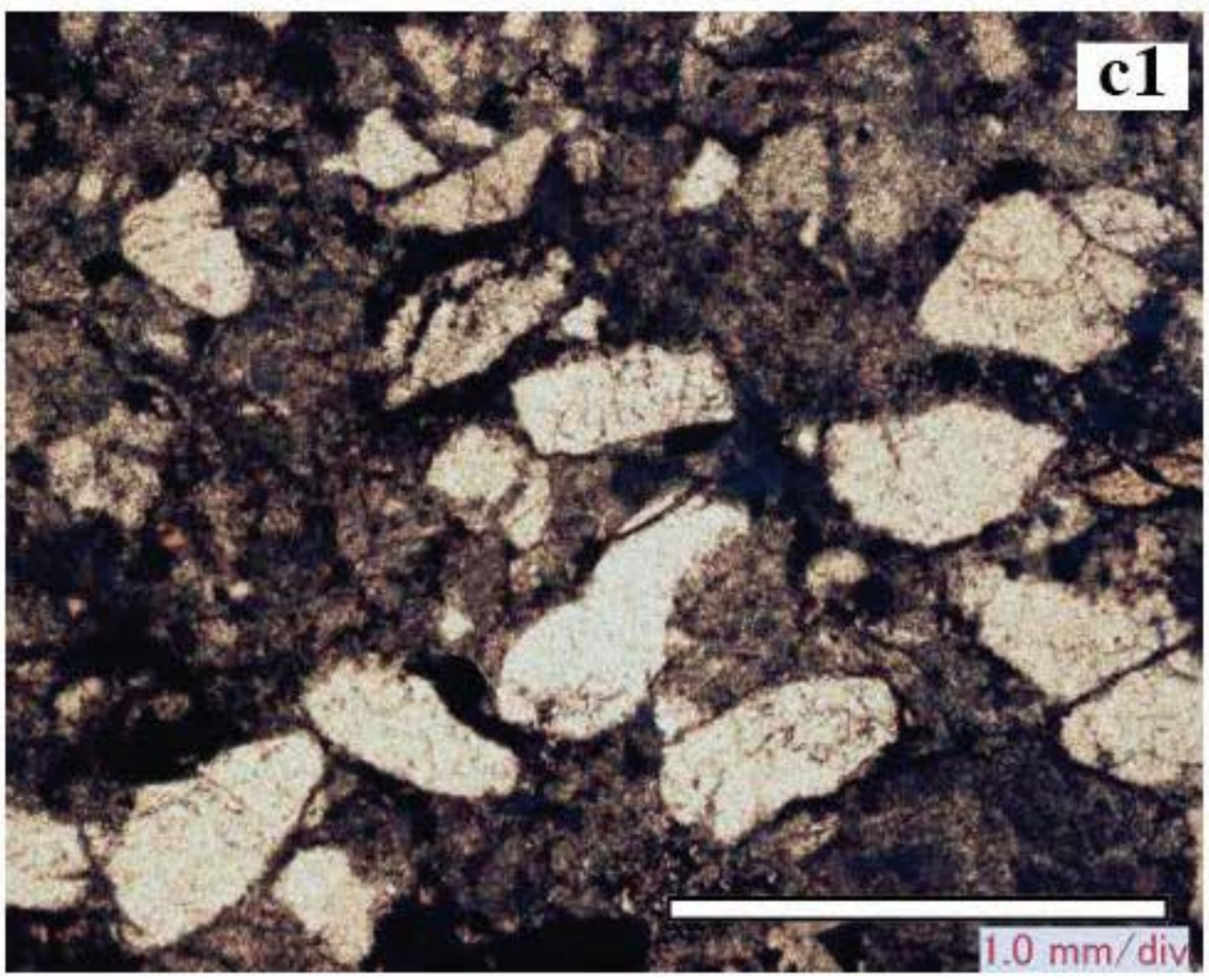
c1
1.0 mm/div

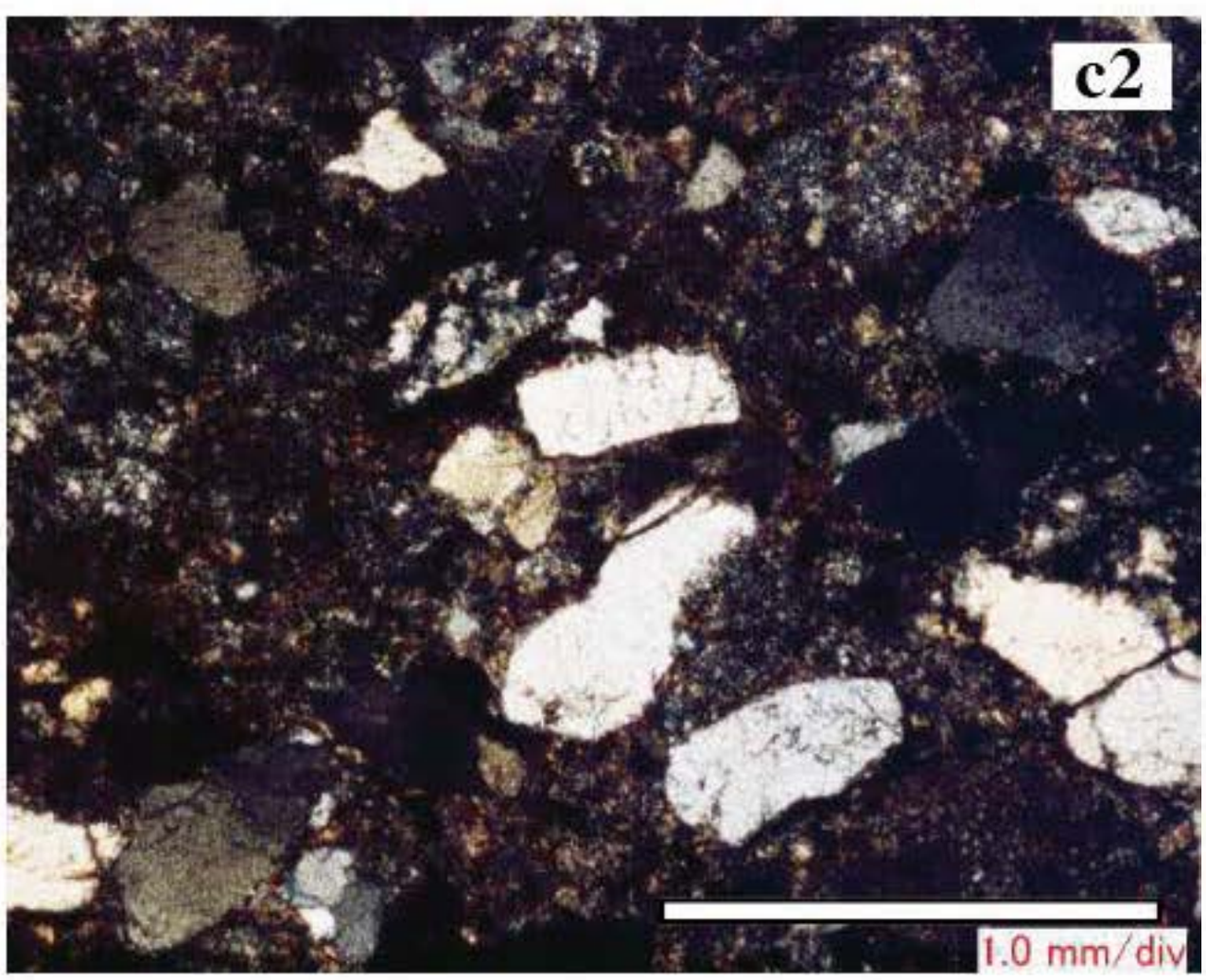
c2
1.0 mm/div

Figure 5

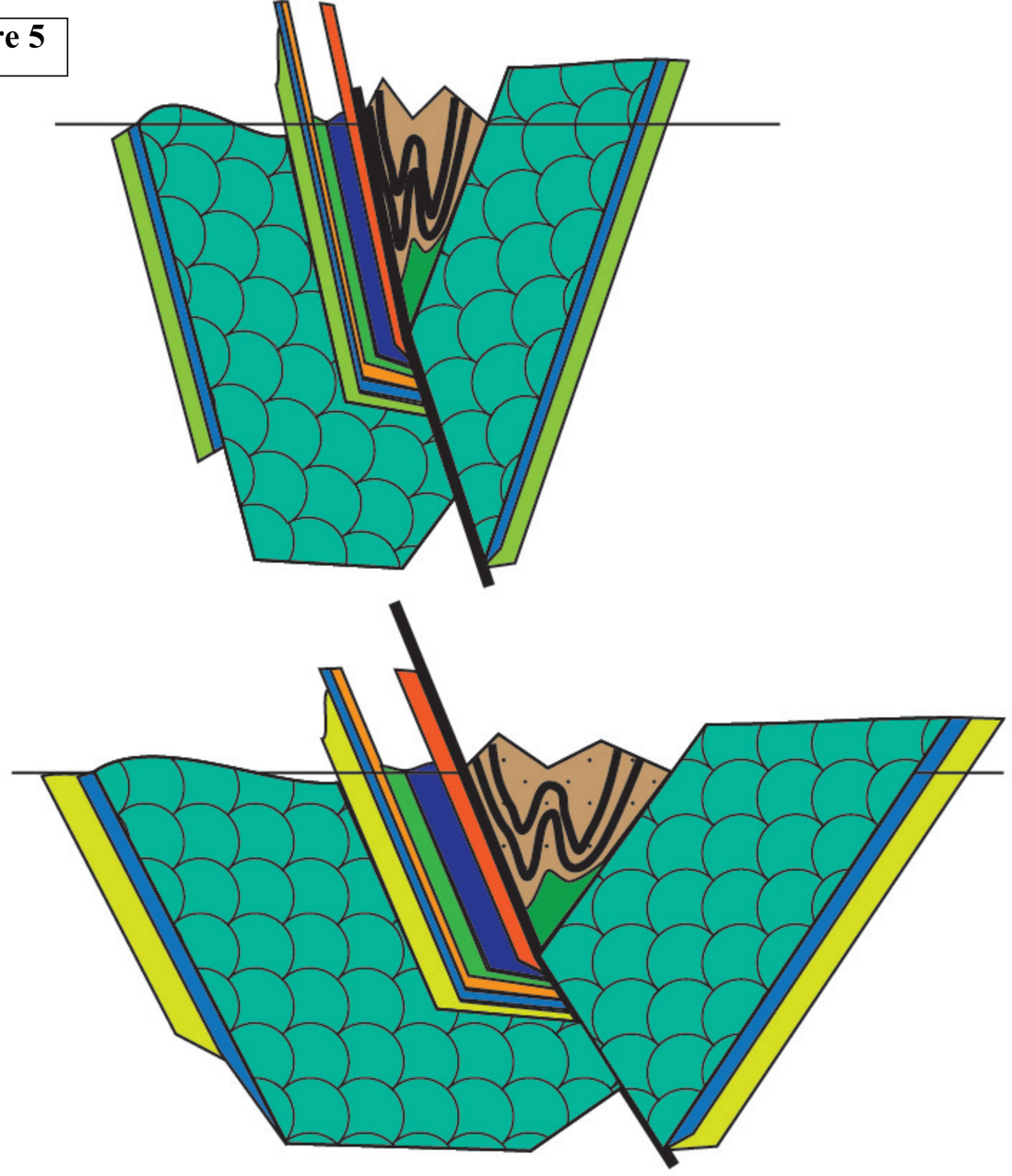

5: Tight folding

During D_2 deformation

4: Fold axis plane deformed (fault)

3: Sedimentation

3060 Ma volcanics

Sixty-Six Hill Member

Black chert fragments

2: Erosion

1: Fold and thrust

Top to northwest thrust

Cleaverville Syncline

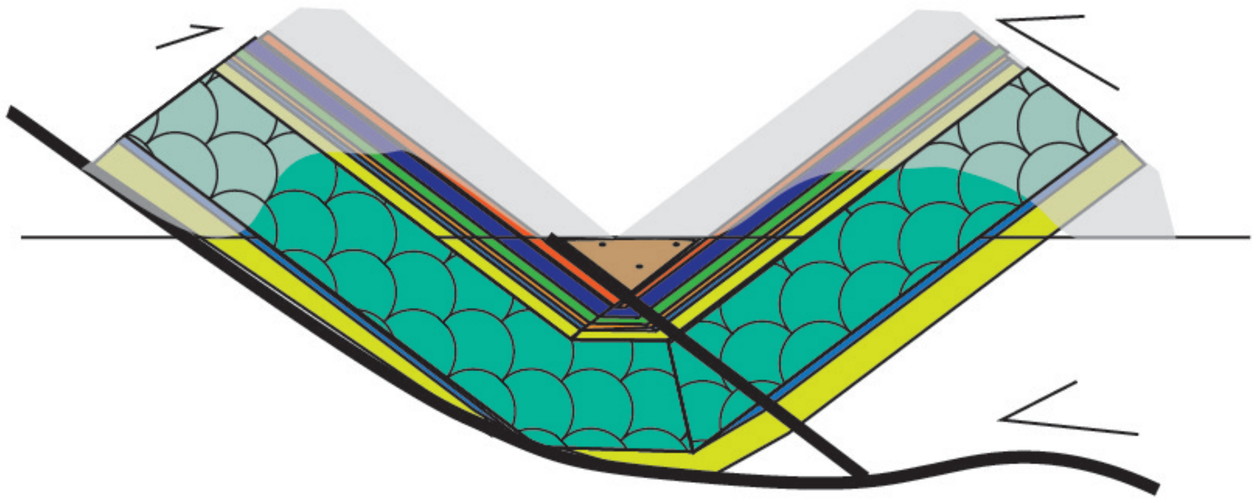

D_1 deformation

Original stratigraphy

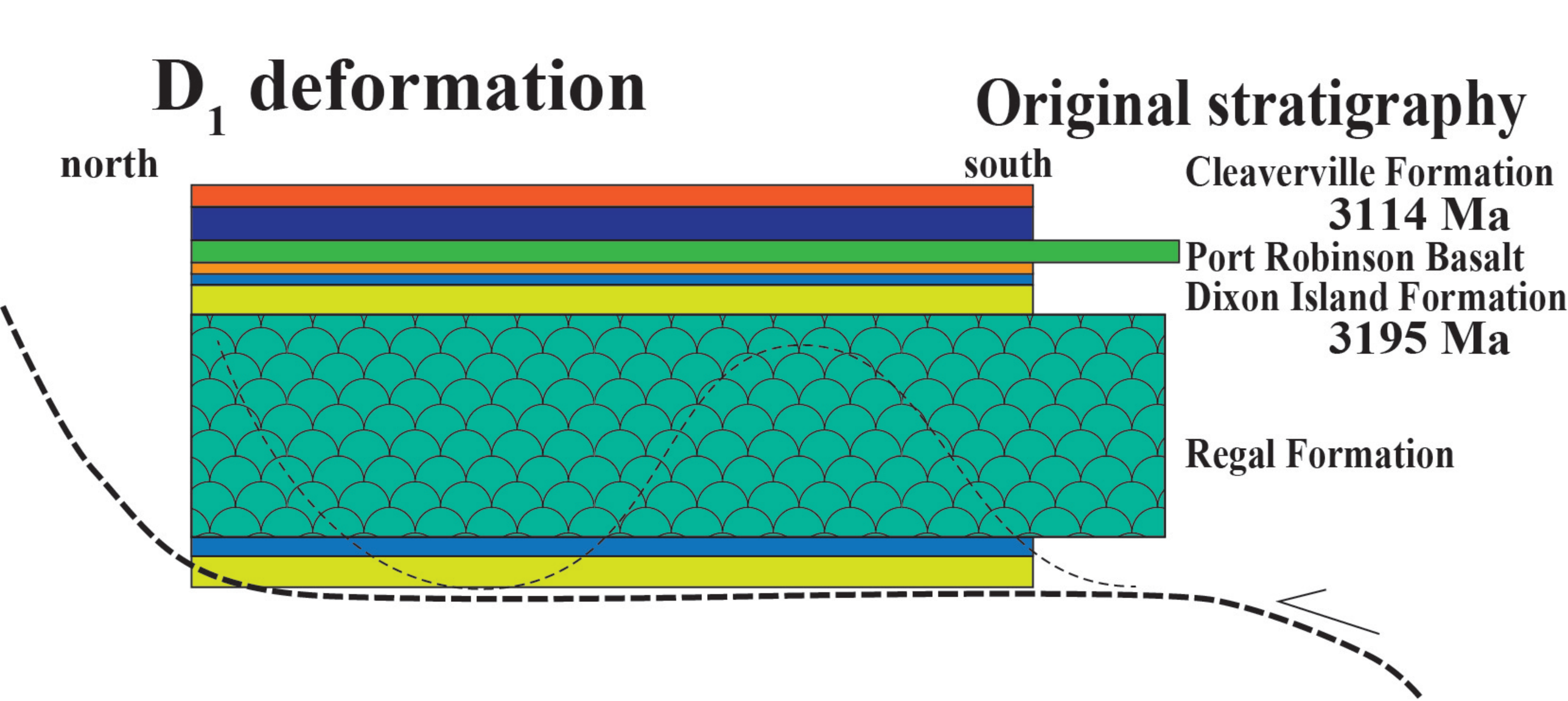

Figure 6

(a)

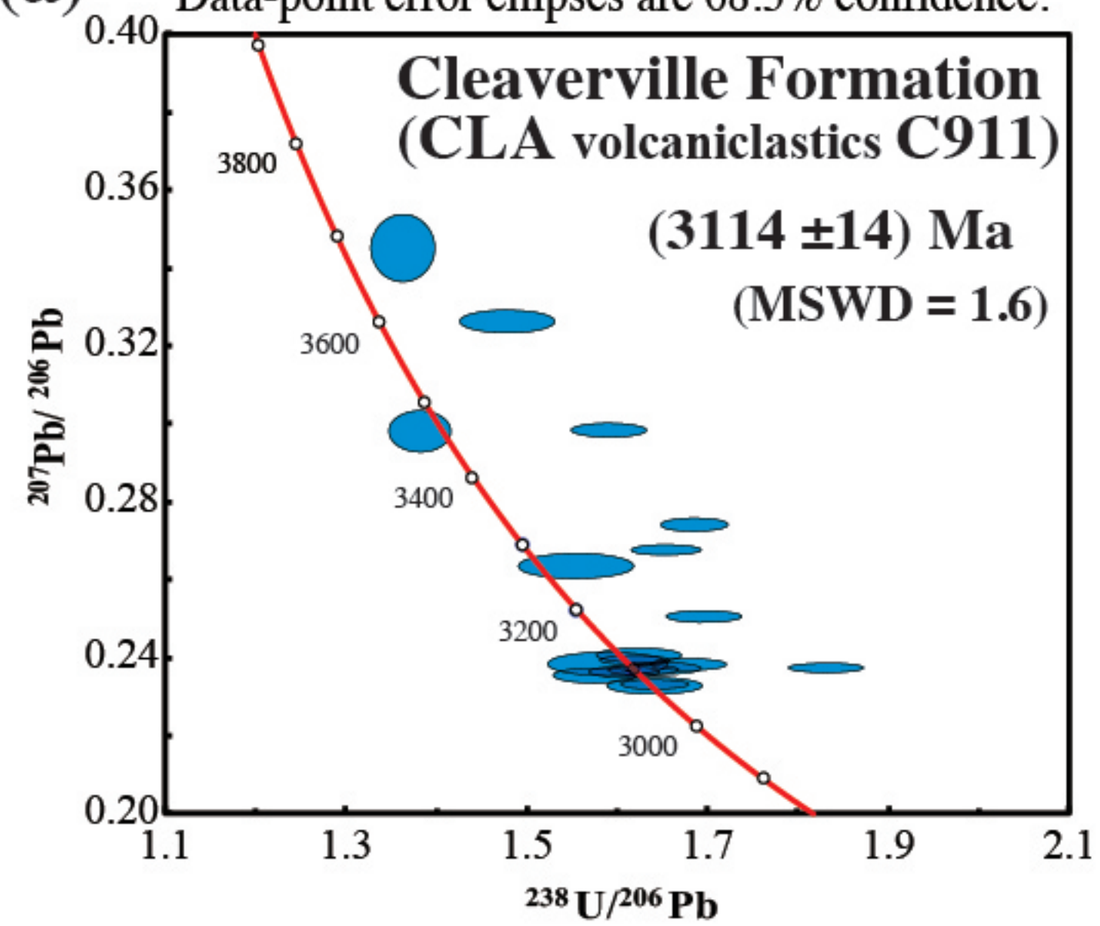

(b) Volcaniclastics (C911)

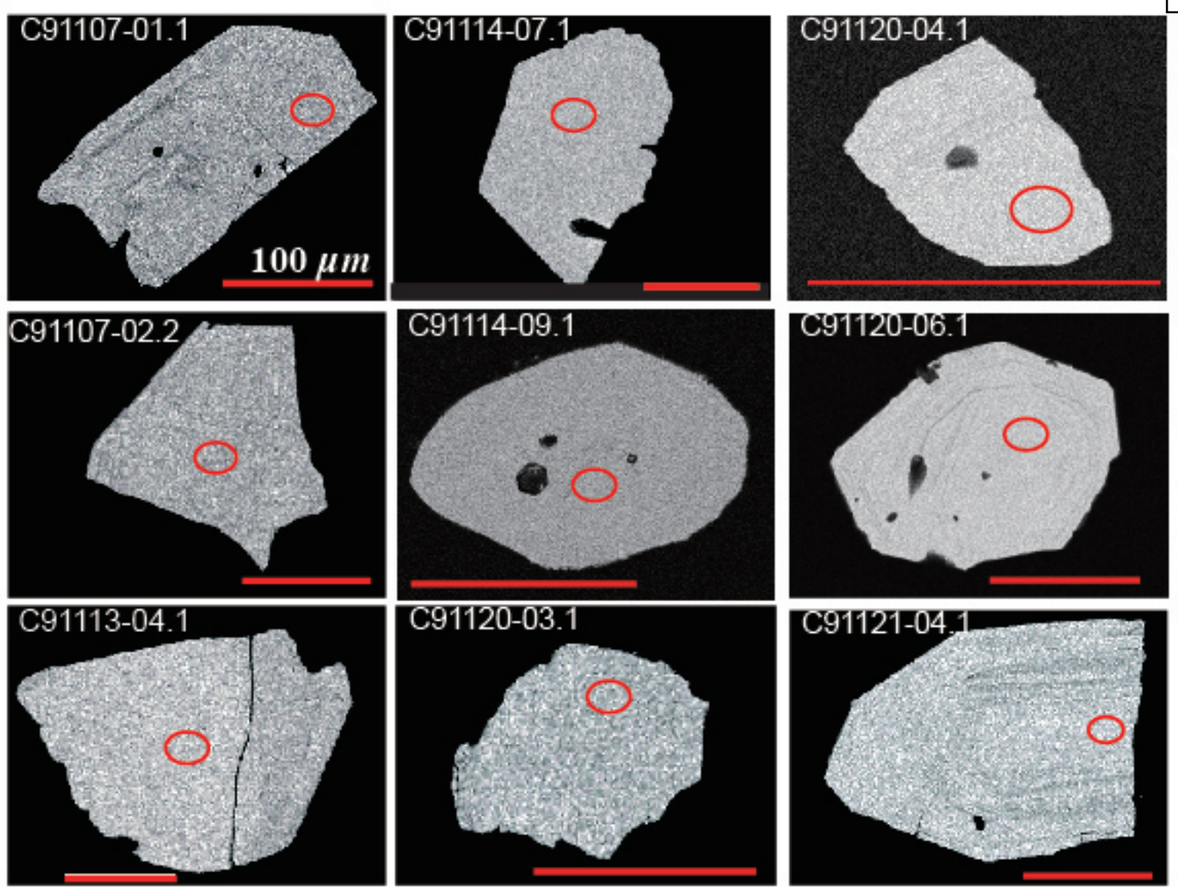

(c)

(d)

D_2 structural map of the coastal Pilbara terrane

Figure 7

Hearsons Cove
Dampier
Walcott Island
Dixon Island
Cleaverville
Point Samson
Karratha Airport
Karratha
Millars Well
Mulataga
Gap Ridge
Bayton
Karratha Industrial Estate
Stove Hill
Prinsep dome
Sholl Shear Zone
0
10 km

LEGEND

- Fortescue Group
- Forty-Four Hill Formation
- Sixty-Six Hill Formation
- Cleaverville Formation
- Dixon Island Formation
- Bedded chert/BIF quartz mylonite
- Pillow lava (amphibolite) Regal/Nickol Well subcomplex
- Strike-slip fault
- Strike-slip normal fault
- Slip direction
- Younging (pillow lava)
- Fold axis (antcline, syncline)

Figure 8

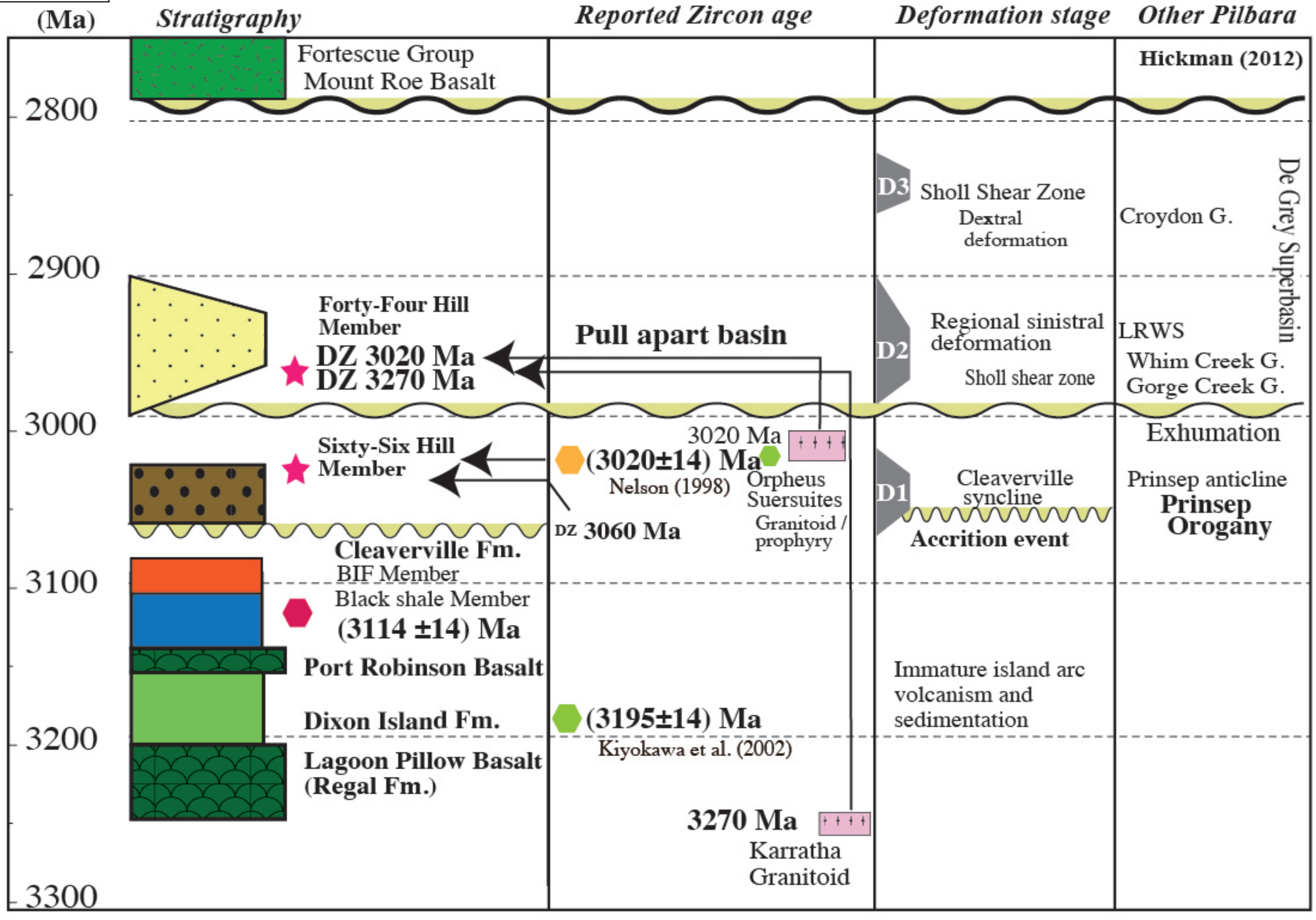
(Ma)
Stratigraphy
Reported Zircon age
Deformation stage
Other Pilbara
Hickman (2012)
Fortescue Group
Mount Roe Basalt
2800
2900
3000
3100
3200
3300
D3
Sholl Shear Zone
Dextral deformation
Croydon G.
De Grey Superbasin
Forty-Four Hill Member
DZ 3020 Ma
DZ 3270 Ma
Pull apart basin
D2
Regional sinistral deformation
Sholl shear zone
LRWS
Whim Creek G.
Gorge Creek G.
Exhumation
Sixty-Six Hill Member
3020 Ma
(3020±14) Ma
Nelson (1998)
Orpheus Suersuites
Granitoid / prophyry
DZ 3060 Ma
D1
Cleaverville syncline
Accrition event
Prinsep anticline
Prinsep Orogany
Cleaverville Fm.
BIF Member
Black shale Member
(3114 ±14) Ma
Port Robinson Basalt
Dixon Island Fm.
Lagoon Pillow Basalt
(Regal Fm.)
Immature island arc volcanism and sedimentation
(3195±14) Ma
Kiyokawa et al. (2002)
3270 Ma
Karratha Granitoid
Sandstone
This study
Volcaniclastics -felsic tuff
This study
Volcaniclastics -felsic tuff
Kiyokawa et al. (2002)
Volcaniclastics -felsic tuff
Nelson (1998)
Granitoid
Nelson (1998) Smith et al., (1998) Kiyokawa et al. (2002)
LRWS : Lalla Rookh-Western Shaw structural corridor
DZ : Detrital zircon G.: Group Fm.: Formation

TABLE 1. U–Pb age data of felsic tuff and sandstone detrital zircon

Sample number	Discordancy	U (ppm)	Th (ppm)	Th/U	$^{206}Pb_{co}$ (%)	$^{207}Pb^*/^{206}Pb^*$			$^{238}U/^{206}Pb^*$			$^{206}Pb^*/^{238}U$ age (Ma)		$^{207}Pb^*$ age
CLA (same rock)														
C91107-01.1		###	60	0.51	0.01	######	±	#####	######	±	#####	3029	± 67	####
C91107-02.1	D	###	348	2.86	0.70	######	±	#####	######	±	#####	1707	± ###	####
C91107-02.2		###	68	0.56	0.01	######	±	#####	######	±	#####	2973	± 65	####
C91107-03.1	D	###	777	2.41	3.70	######	±	#####	######	±	#####	1463	± 30	####
C91107-04.1	D	###	168	1.06	0.45	######	±	#####	######	±	#####	2464	± 53	####
C91113-01.1		###	174	0.89	0.06	######	±	#####	######	±	#####	3074	± 58	####
C91113-02.1	D	###	117	0.89	0.09	######	±	#####	######	±	#####	2925	± 62	####
C91113-03.1		###	39	0.34	0.08	######	±	#####	######	±	#####	3297	± 71	####
C91113-04.1		###	304	1.73	0.06	######	±	#####	######	±	#####	3143	± 62	####
C91114-01.1	D	###	978	2.31	0.55	######	±	#####	######	±	#####	2132	± 37	####
C91114-02.1		###	166	0.70	0.05	######	±	#####	######	±	#####	3491	± ###	####
C91114-03.1	D	###	694	1.66	0.23	######	±	#####	######	±	#####	1678	± 29	####
C91114-04.1	D	###	679	2.30	0.21	######	±	#####	######	±	#####	1979	± 36	####
C91114-05.1		###	54	0.48	0.13	######	±	#####	######	±	#####	3567	± 77	####
C91114-06.1		39	33	0.88	0.14	######	±	#####	######	±	#####	3349	± ###	####
C91114-07.1		90	229	2.64	####	######	±	#####	######	±	#####	3067	± 80	####
C91114-08.1	D	###	299	2.62	0.31	######	±	#####	######	±	#####	2086	± 50	####
C91114-09.1		###	287	1.57	0.07	######	±	#####	######	±	#####	3030	± 63	####
C91114-09.2	D	55	27	0.50	0.00	######	±	#####	######	±	#####	2254	± 81	####
C91114-10.1	D	###	###	####	0.81	######	±	#####	######	±	#####	1391	± 41	####
C91114-11.1	D	###	159	0.68	0.06	######	±	#####	######	±	#####	3249	± 63	####
C91119-01.1	D	###	###	0.95	0.35	######	±	#####	######	±	#####	817	± 14	####
C91119-01.2	D	###	###	1.65	0.26	######	±	#####	######	±	#####	874	± 15	####
C91119-02.1	D	###	35	0.19	0.48	######	±	#####	######	±	#####	2539	± 54	####
C91119-03.1	D	###	365	1.85	0.14	######	±	#####	######	±	#####	2398	± 50	####
C91119-04.1	D	###	317	2.27	0.08	######	±	#####	######	±	#####	2493	± 52	####
C91119-05.1	D	###	329	1.49	1.15	######	±	#####	######	±	#####	2075	± 46	####
C91119-06.1	D	###	554	1.76	0.15	######	±	#####	######	±	#####	2473	± 60	####
C91120-01.1	D	51	64	1.29	0.35	######	±	#####	######	±	#####	2582	± 90	####
C91120-03.1		34	38	1.17	####	######	±	#####	######	±	#####	3020	± ###	####
C91120-04.1		###	49	0.49	0.11	######	±	#####	######	±	#####	3241	± 82	####
C91120-05.1	D	###	297	0.98	0.10	######	±	#####	######	±	#####	2565	± 48	####

C91120-06.1		72	67	0.96	0.05	######	±	#####	######	±	#####	3018	±	89	####
C91121-02.1		###	83	0.48	0.03	######	±	#####	######	±	#####	3153	±	63	####
C91121-03.1	D	###	874	1.63	0.29	######	±	#####	######	±	#####	1479	±	32	####
C91121-04.1		###	79	0.44	0.00	######	±	#####	######	±	#####	3160	±	62	####
C91121-05.1	D	###	100	0.55	0.07	######	±	#####	######	±	#####	2808	±	54	####
C91121-06.1	D	###	430	2.14	0.17	######	±	#####	######	±	#####	2257	±	44	####
C91123-01.1	D	###	374	1.16	0.67	######	±	#####	######	±	#####	2385	±	41	####
C91123-02.1	D	###	###	2.49	0.22	######	±	#####	######	±	#####	1661	±	29	####
C91123-03.1	D	###	###	3.34	0.31	######	±	#####	######	±	#####	1693	±	28	####
C91126-01.1	D	53	49	0.97	####	######	±	#####	######	±	#####	3358	±	###	####
C91126-02.1	D	###	###	2.99	0.30	######	±	#####	######	±	#####	1945	±	34	####
C91127-01.1	D	###	256	0.98	0.77	######	±	#####	######	±	#####	2904	±	53	####
C91127-02.1	D	###	595	0.93	2.58	######	±	#####	######	±	#####	877	±	16	####
C91127-03.1		###	155	0.76	0.01	######	±	#####	######	±	#####	3037	±	58	####

Forty-Four Hill		U	Th	Th/U	$^{206}Pb_{co}$	$^{207}Pb^*/^{206}Pb^*$			$^{238}U/^{206}Pb^*$			$^{206}Pb^*/^{238}U$			$^{207}Pb^*$
100912-28		(ppm)	(ppm)		(%)							age (Ma)			age
C91228-01.1	D	###	110	0.24	3.31	######	±	#####	######	±	#####	1606	±	20	####
C91228-02.1		55	47	0.89	0.10	######	±	#####	######	±	#####	3181	±	57	####
C91228-03.1	D	###	736	0.76	3.37	######	±	#####	######	±	#####	1012	±	12	####
C91228-04.1	D	###	116	0.32	2.03	######	±	#####	######	±	#####	1860	±	23	####
C91228-05.1	D	###	978	1.54	3.93	######	±	#####	######	±	#####	1105	±	14	####
C91228-06.1		###	30	0.26	0.00	######	±	#####	######	±	#####	3009	±	43	####
C91228-07.1		###	27	0.12	0.07	######	±	#####	######	±	#####	2862	±	36	####
C91228-08.1		###	164	0.69	0.06	######	±	#####	######	±	#####	3137	±	38	####
C91228-09.1	D	###	194	0.49	2.52	######	±	#####	######	±	#####	1621	±	20	####
C91228-10.1	D	###	268	1.20	2.26	######	±	#####	######	±	#####	2047	±	27	####
C91228-11.1	D	###	269	0.81	1.20	######	±	#####	######	±	#####	2079	±	25	####
C91228-12.1		###	85	0.52	0.07	######	±	#####	######	±	#####	2951	±	39	####
C91228-13.1		###	36	0.23	0.01	######	±	#####	######	±	#####	2939	±	39	####
C91228-14.1	D	###	591	1.29	2.81	######	±	#####	######	±	#####	1596	±	21	####
C91228-15.1		###	51	0.31	0.03	######	±	#####	######	±	#####	3014	±	40	####
C91228-17.1		###	26	0.26	0.10	######	±	#####	######	±	#####	2951	±	44	####
C91228-18.1		###	144	0.68	0.03	######	±	#####	######	±	#####	3259	±	40	####
C91228-16.1	D	###	130	0.37	1.82	######	±	#####	######	±	#####	2016	±	25	####
C91228-19.1	D	###	###	2.55	2.22	######	±	#####	######	±	#####	1675	±	20	####

C91228-20.1	D	###	237	0.53	2.26	######	±	#####	######	±	#####	1728	±	21	####
C91228-21.1		69	76	1.13	0.10	######	±	#####	######	±	#####	3208	±	52	####
C91228-22.1	D	###	137	0.46	2.01	######	±	#####	######	±	#####	1684	±	21	####
C91228-23.1	D	###	649	0.99	3.19	######	±	#####	######	±	#####	997	±	13	####
C91228-24.1	D	###	116	0.42	0.40	######	±	#####	######	±	#####	2717	±	33	####
C91228-25.1	D	###	175	1.04	0.29	######	±	#####	######	±	#####	3142	±	41	####
C91228-26.1	D	###	193	0.94	0.14	######	±	#####	######	±	#####	2718	±	35	####
C91228-27.1	D	###	65	0.23	0.23	######	±	#####	######	±	#####	2697	±	36	####
C91228-28.1	D	###	339	0.54	2.39	######	±	#####	######	±	#####	1372	±	17	####
C91228-29.1		82	102	1.29	0.11	######	±	#####	######	±	#####	3198	±	51	####
C91228-30.1	D	###	952	0.91	5.45	######	±	#####	######	±	#####	927	±	12	####
C91228-31.1		###	140	1.32	0.03	######	±	#####	######	±	#####	3199	±	49	####
C91228-32.1		###	42	0.28	0.03	######	±	#####	######	±	#####	2926	±	42	####
C91228-33.1	D	###	104	0.43	0.67	######	±	#####	######	±	#####	2407	±	30	####
C91228-34.1	D	###	###	1.77	4.52	######	±	#####	######	±	#####	1074	±	14	####
C91228-35.1	D	###	115	0.30	1.81	######	±	#####	######	±	#####	1724	±	58	####
C91228-36.1	D	###	121	0.62	0.34	######	±	#####	######	±	#####	2021	±	27	####
C91228-37.1		###	59	0.50	0.02	######	±	#####	######	±	#####	3046	±	42	####
C91228-37.2	D	###	78	0.70	0.41	######	±	#####	######	±	#####	2681	±	40	####
C91228-38.1	D	###	792	1.32	2.85	######	±	#####	######	±	#####	1152	±	15	####
C91228-39.1		###	66	0.43	0.08	######	±	#####	######	±	#####	3183	±	44	####
C91228-40.1		56	45	0.82	0.20	######	±	#####	######	±	#####	3113	±	57	####
C91228-41.1	D	###	282	0.48	3.10	######	±	#####	######	±	#####	1428	±	18	####
C91228-42.1		###	58	0.26	0.20	######	±	#####	######	±	#####	2934	±	37	####
C91228-43.1	D	###	148	0.58	0.99	######	±	#####	######	±	#####	2248	±	29	####
C91228-44.1		###	176	0.67	0.19	######	±	#####	######	±	#####	2874	±	36	####
C91228-44.2		###	135	0.64	0.01	######	±	#####	######	±	#####	2992	±	40	####
C91228-45.1		###	41	0.30	0.01	######	±	#####	######	±	#####	2904	±	42	####
C91228-45.2	D	###	79	0.37	1.09	######	±	#####	######	±	#####	2052	±	29	####
C91228-46.1	D	###	112	0.42	0.62	######	±	#####	######	±	#####	2236	±	29	####
C91228-47.1	D	###	65	0.42	0.16	######	±	#####	######	±	#####	2726	±	41	####
C91228-48.1	D	###	264	0.99	1.27	######	±	#####	######	±	#####	2069	±	27	####
C91228-48.2	D	###	133	0.48	0.61	######	±	#####	######	±	#####	2359	±	30	####
C91228-49.1	D	###	128	0.53	0.54	######	±	#####	######	±	#####	2625	±	34	####
C91228-50.1	D	###	423	0.83	2.47	######	±	#####	######	±	#####	1742	±	21	####
C91228-51.1	D	###	172	0.34	2.43	######	±	#####	######	±	#####	1549	±	19	####

C91228-52.1	D	###	80	0.29	0.33	######	±	#####	######	±	#####	2753	± 35	####
C91228-53.1	D	###	276	0.64	1.38	######	±	#####	######	±	#####	1918	± 28	####
C91228-55.1	D	###	194	0.40	2.06	######	±	#####	######	±	#####	1819	± 23	####
C91228-56.1	D	###	55	0.26	0.52	######	±	#####	######	±	#####	2707	± 37	####
C91228-57.1	D	###	245	0.59	2.33	######	±	#####	######	±	#####	1917	± 24	####
C91228-58.1		###	39	0.33	0.46	######	±	#####	######	±	#####	2858	± 44	####
C91228-59.1		###	37	0.27	0.02	######	±	#####	######	±	#####	2952	± 44	####
C91228-60.1		###	41	0.37	0.02	######	±	#####	######	±	#####	2938	± 46	####
C91228-61.1	D	###	144	0.44	1.75	######	±	#####	######	±	#####	2210	± 28	####

Sixty-Six Hill M	U	Th	Th/U	$^{206}Pb_{co}$	$^{207}Pb^*/^{206}Pb^*$			$^{238}U/^{206}Pb^*$			$^{206}Pb^*/^{238}U$		$^{207}Pb^*$
100912-14	(ppm)	(ppm)		(%)							age (Ma)		age
C91214-01.1	###	512	1.71	0.57	######	±	#####	######	±	#####	2852	± 31	####
C91214-01.2	###	108	0.47	0.04	######	±	#####	######	±	#####	3108	± 34	####
C91214-02.1	94	60	0.66	0.10	######	±	#####	######	±	#####	3079	± 47	####
C91214-03.1	83	56	0.70	0.04	######	±	#####	######	±	#####	3144	± 41	####
C91214-04.1	###	158	0.64	0.04	######	±	#####	######	±	#####	3078	± 34	####
C91214-05.1	90	48	0.55	0.14	######	±	#####	######	±	#####	3166	± 42	####
C91214-06.1	95	62	0.67	0.19	######	±	#####	######	±	#####	3116	± 39	####
C91214-07.1	###	115	0.98	0.10	######	±	#####	######	±	#####	3054	± 37	####
C91214-08.1	###	75	0.68	–	######	±	#####	######	±	#####	3119	± 39	####
C91214-09.1	###	144	0.57	0.07	######	±	#####	######	±	#####	3069	± 34	####
C91214-10.1	###	238	0.82	0.19	######	±	#####	######	±	#####	2994	± 32	####
C91214-11.1	###	169	1.30	0.10	######	±	#####	######	±	#####	3130	± 39	####
C91214-12.1	###	115	0.59	0.24	######	±	#####	######	±	#####	3018	± 34	####
C91214-13.1	###	167	0.63	0.18	######	±	#####	######	±	#####	3011	± 37	####
C91214-14.1	###	93	0.40	0.10	######	±	#####	######	±	#####	3081	± 41	####
C91214-15.1	###	101	0.69	5.00	######	±	#####	######	±	#####	2923	± 42	####
C91214-16.1	###	47	0.22	0.08	######	±	#####	######	±	#####	3141	± 44	####
C91214-17.1	99	69	0.72	0.16	######	±	#####	######	±	#####	3028	± 68	####
C91214-18.1	###	365	1.05	0.28	######	±	#####	######	±	#####	3049	± 33	####
C91214-19.1	###	91	0.48	0.05	######	±	#####	######	±	#####	3085	± 36	####
C91214-20.1	99	76	0.79	0.12	######	±	#####	######	±	#####	3495	± 44	####
C91214-21.1	95	56	0.61	0.26	######	±	#####	######	±	#####	3216	± 44	####
C91214-22.1	###	140	1.09	–	######	±	#####	######	±	#####	3149	± 39	####
C91214-23.1	###	155	0.60	0.04	######	±	#####	######	±	#####	3104	± 34	####

C91214-24.1	###	71	0.58	–	######	±	#####	######	±	#####	3257	± 40	####
C91214-25.1	###	144	0.55	0.05	######	±	#####	######	±	#####	3097	± 34	####
C91214-26.1	###	190	1.24	0.27	######	±	#####	######	±	#####	2932	± 36	####
C91214-27.1	###	211	1.13	0.12	######	±	#####	######	±	#####	3268	± 43	####
C91214-28.1	69	37	0.55	0.27	######	±	#####	######	±	#####	3122	± 47	####
C91214-29.1	55	17	0.35	–	######	±	#####	######	±	#####	3076	± 58	####
C91214-30.1	95	57	0.63	0.12	######	±	#####	######	±	#####	3150	± 44	####
C91214-31.1	72	37	0.54	0.01	######	±	#####	######	±	#####	3107	± 55	####
C91214-32.1	###	102	0.78	0.09	######	±	#####	######	±	#####	3121	± 39	####
C91214-33.1	61	33	0.56	0.20	######	±	#####	######	±	#####	3163	± 48	####
C91214-34.1	###	103	0.44	0.02	######	±	#####	######	±	#####	3106	± 35	####
C91214-35.1	###	246	0.84	0.12	######	±	#####	######	±	#####	3009	± 35	####
C91214-36.1	###	126	0.96	0.07	######	±	#####	######	±	#####	3048	± 38	####
C91214-37.1	###	124	0.77	0.04	######	±	#####	######	±	#####	3102	± 36	####
C91214-38.1	###	78	0.76	0.13	######	±	#####	######	±	#####	3068	± 39	####
C91214-39.1	###	209	0.67	0.05	######	±	#####	######	±	#####	3082	± 33	####
C91214-40.1	###	128	0.53	–	######	±	#####	######	±	#####	3004	± 33	####
C91214-41.1	###	150	0.63	0.00	######	±	#####	######	±	#####	3731	± 40	####
C91214-42.1	30	20	0.67	0.41	######	±	#####	######	±	#####	3091	± 57	####
C91214-43.1	94	54	0.60	0.08	######	±	#####	######	±	#####	3053	± 51	####
C91214-44.1	###	180	0.75	0.07	######	±	#####	######	±	#####	3096	± 39	####
C91214-45.1	###	157	0.64	0.04	######	±	#####	######	±	#####	3098	± 34	####
C91214-46.1	87	55	0.65	0.06	######	±	#####	######	±	#####	3207	± 42	####
C91214-47.1	84	42	0.51	0.17	######	±	#####	######	±	#####	3113	± 42	####
C91214-48.1	###	122	0.54	0.02	######	±	#####	######	±	#####	3137	± 35	####
C91214-49.1	###	198	0.79	0.03	######	±	#####	######	±	#####	3171	± 35	####
C91214-50.1	98	51	0.54	0.07	######	±	#####	######	±	#####	3111	± 40	####
C91214-51.1	###	137	0.71	–	######	±	#####	######	±	#####	3280	± 37	####
C91214-52.1	###	103	0.52	0.08	######	±	#####	######	±	#####	3049	± 39	####
C91214-53.1	###	237	0.72	0.01	######	±	#####	######	±	#####	3084	± 33	####
C91214-54.1	###	133	0.65	0.02	######	±	#####	######	±	#####	3045	± 34	####
C91214-55.1	###	60	0.54	0.07	######	±	#####	######	±	#####	3132	± 39	####
C91214-56.1	###	202	0.80	0.05	######	±	#####	######	±	#####	3065	± 34	####
C91214-57.1	###	116	0.54	0.00	######	±	#####	######	±	#####	3166	± 35	####
C91214-58.1	###	188	0.68	0.06	######	±	#####	######	±	#####	3080	± 33	####
C91214-59.1	###	141	0.55	0.03	######	±	#####	######	±	#####	3177	± 35	####

C91214-60.1	###	98	0.83	0.01	######	±	#####	######	±	#####	3089	± 38	####
C91214-61.1	###	18	0.19	0.03	######	±	#####	######	±	#####	3462	± 44	####
C91214-62.1	###	153	0.90	0.04	######	±	#####	######	±	#####	3100	± 36	####
C91214-63.1	###	123	0.63	0.07	######	±	#####	######	±	#####	3116	± 35	####
C91214-64.1	###	93	0.74	0.05	######	±	#####	######	±	#####	3066	± 43	####
C91214-65.1	###	94	0.62	0.09	######	±	#####	######	±	#####	3310	± 39	####
C91214-66.1	###	78	0.44	0.06	######	±	#####	######	±	#####	3089	± 42	####
C91214-67.1	###	104	0.68	–	######	±	#####	######	±	#####	3094	± 37	####
C91214-68.1	###	146	0.54	–	######	±	#####	######	±	#####	3116	± 34	####
C91214-69.1	###	111	0.57	0.25	######	±	#####	######	±	#####	3014	± 34	####
C91214-70.1	###	60	0.63	0.09	######	±	#####	######	±	#####	3188	± 49	####
C91214-71.1	###	70	0.54	0.12	######	±	#####	######	±	#####	3028	± 37	####
C91214-72.1	###	103	0.47	0.01	######	±	#####	######	±	#####	3096	± 34	####
C91214-73.1	85	53	0.64	0.10	######	±	#####	######	±	#####	3181	± 42	####
C91214-74.1	###	201	0.73	0.06	######	±	#####	######	±	#####	3303	± 35	####
C91214-75.1	97	56	0.59	–	######	±	#####	######	±	#####	3133	± 42	####
C91214-76.1	###	136	0.56	0.06	######	±	#####	######	±	#####	2979	± 32	####
C91214-77.1	71	43	0.63	0.10	######	±	#####	######	±	#####	3080	± 43	####
C91214-78.1	###	137	0.78	0.10	######	±	#####	######	±	#####	3050	± 35	####
C91214-79.1	###	174	0.61	0.04	######	±	#####	######	±	#####	3104	± 34	####
C91214-80.1	###	251	0.99	0.05	######	±	#####	######	±	#####	3424	± 37	####
C91214-81.1	90	45	0.52	–	######	±	#####	######	±	#####	3050	± 41	####
C91214-82.1	74	53	0.74	0.10	######	±	#####	######	±	#####	3183	± 47	####
C91214-83.1	###	259	0.72	0.06	######	±	#####	######	±	#####	3050	± 37	####
C91214-84.1	###	135	0.69	0.02	######	±	#####	######	±	#####	3324	± 38	####
C91214-85.1	###	279	0.80	0.06	######	±	#####	######	±	#####	3050	± 33	####
C91214-86.1	###	104	0.70	0.08	######	±	#####	######	±	#####	3074	± 37	####
C91214-87.1	76	41	0.56	0.12	######	±	#####	######	±	#####	3062	± 43	####
C91214-88.1	###	177	0.57	0.11	######	±	#####	######	±	#####	3019	± 35	####

Sixty-Six Hill M	U	Th	Th/U	$^{206}Pb_{co}$	$^{207}Pb^*/^{206}Pb^*$			$^{238}U/^{206}Pb^*$			$^{206}Pb^*/^{238}U$		$^{207}Pb^*$
100912-15	(ppm)	(ppm)		(%)							age (Ma)		age
C91215-2.1	###	206	1.05	0.16	######	±	#####	######	±	#####	3235	± 24	####
C91215-26.1	70	57	0.85	0.03	######	±	#####	######	±	#####	3055	± 35	####

C91215-8.1		13	9	0.69	0.42	######	±	#####	######	±	#####	3176	± 77	####
C91215-60.1	D	###	285	0.52	2.08	######	±	#####	######	±	#####	1669	± 11	####
C91215-85.1		###	116	0.59	0.01	######	±	#####	######	±	#####	3102	± 23	####
C91215-161.1		###	141	1.15	0.01	######	±	#####	######	±	#####	3319	± 30	####
C91215-314.1		###	67	0.58	–	######	±	#####	######	±	#####	3156	± 29	####
C91215-286.1		###	134	1.01	0.03	######	±	#####	######	±	#####	3267	± 28	####
C91215-320.1		###	115	0.52	0.01	######	±	#####	######	±	#####	3047	± 22	####
C91215-328.1		###	130	0.76	0.02	######	±	#####	######	±	#####	3097	± 25	####
C91215-156.1		39	16	0.43	0.15	######	±	#####	######	±	#####	2977	± 44	####
C91215-59.1		###	99	0.71	0.04	######	±	#####	######	±	#####	3227	± 28	####
C91215-410.1		81	47	0.61	0.06	######	±	#####	######	±	#####	3085	± 33	####
C91215-110.1		###	126	0.50	0.02	######	±	#####	######	±	#####	3037	± 21	####
C91215-80.1		74	40	0.56	0.11	######	±	#####	######	±	#####	3051	± 35	####
C91215-381.1		###	68	0.46	0.01	######	±	#####	######	±	#####	3068	± 26	####
C91215-453.1		93	78	0.86	0.03	######	±	#####	######	±	#####	3077	± 32	####
C91215-425.1		###	68	0.49	0.06	######	±	#####	######	±	#####	3010	± 26	####
C91215-480.1		40	17	0.43	0.17	######	±	#####	######	±	#####	3058	± 45	####
C91215-509.1		###	121	0.59	–	######	±	#####	######	±	#####	3121	± 23	####
C91215-436.1		###	90	0.53	–	######	±	#####	######	±	#####	3262	± 26	####
C91215-437.1		###	57	0.51	0.02	######	±	#####	######	±	#####	3488	± 32	####
C91215-438.1		95	52	0.57	0.02	######	±	#####	######	±	#####	3121	± 32	####
C91215-392.1		###	62	0.44	0.10	######	±	#####	######	±	#####	3104	± 27	####
C91215-414.1		15	10	0.68	–	######	±	#####	######	±	#####	3228	± 76	####
C91215-470.1		29	46	1.62	0.03	######	±	#####	######	±	#####	3319	± 57	####
C91215-349.1		###	140	0.60	0.02	######	±	#####	######	±	#####	3085	± 22	####
C91215-63.1		30	14	0.46	–	######	±	#####	######	±	#####	3163	± 55	####
C91215-86.1		###	73	0.62	0.04	######	±	#####	######	±	#####	3117	± 29	####
C91215-212.1		###	85	0.85	–	######	±	#####	######	±	#####	3123	± 31	####
C91215-211.1		###	200	0.96	0.03	######	±	#####	######	±	#####	3186	± 24	####
C91215-209.1		###	144	0.69	0.00	######	±	#####	######	±	#####	3442	± 25	####
C91215-165.1		###	162	0.62	0.00	######	±	#####	######	±	#####	3067	± 21	####
C91215-166.1		###	68	0.63	–	######	±	#####	######	±	#####	3103	± 29	####
C91215-119.1		###	100	0.57	–	######	±	#####	######	±	#####	3097	± 24	####
C91215-87.1		###	155	0.43	0.07	######	±	#####	######	±	#####	3097	± 19	####
C91215-48.1		###	130	0.50	0.01	######	±	#####	######	±	#####	3052	± 20	####
C91215-377.1		###	136	0.46	0.00	######	±	#####	######	±	#####	3063	± 20	####

C91215-356.1	91	51	0.58	–	######	±	#####	######	±	#####	3152	± 33	####
C91215-355.1	###	98	0.74	0.06	######	±	#####	######	±	#####	3101	± 27	####
C91215-357.1	###	53	0.52	0.05	######	±	#####	######	±	#####	3100	± 30	####
C91215-427.1	56	34	0.62	0.02	######	±	#####	######	±	#####	3030	± 39	####
C91215-454.1	###	94	0.64	–	######	±	#####	######	±	#####	3115	± 26	####
C91215-426.1	###	159	0.68	–	######	±	#####	######	±	#####	3073	± 22	####
C91215-468.1	###	132	0.82	–	######	±	#####	######	±	#####	3078	± 25	####
C91215-500.1	###	208	0.75	0.04	######	±	#####	######	±	#####	3248	± 21	####
C91215-444.1	67	38	0.58	0.06	######	±	#####	######	±	#####	3099	± 36	####
C91215-445.1	###	129	0.52	–	######	±	#####	######	±	#####	3174	± 22	####
C91215-177.1	###	97	0.48	0.00	######	±	#####	######	±	#####	3109	± 23	####
C91215-252.1	###	72	0.63	0.05	######	±	#####	######	±	#####	3084	± 28	####
C91215-95.1	###	207	0.99	0.09	######	±	#####	######	±	#####	2947	± 21	####
C91215-352.1	###	156	0.66	–	######	±	#####	######	±	#####	3063	± 21	####
C91215-200.1	###	78	0.69	–	######	±	#####	######	±	#####	3146	± 29	####
C91215-204.1	###	65	0.62	–	######	±	#####	######	±	#####	3055	± 28	####
C91215-247.1	###	118	0.49	0.04	######	±	#####	######	±	#####	3073	± 21	####
C91215-215.1	###	60	0.61	0.06	######	±	#####	######	±	#####	3134	± 29	####
C91215-270.1 D	###	###	4.05	2.77	######	±	#####	######	±	#####	1832	± 11	####
C91215-55.1 D	###	350	1.36	0.69	######	±	#####	######	±	#####	2474	± 17	####
C91215-366.1	23	14	0.66	–	######	±	#####	######	±	#####	3155	± 58	####
C91215-523.1	63	34	0.56	–	######	±	#####	######	±	#####	3112	± 37	####
C91215-50.1	###	95	0.55	0.02	######	±	#####	######	±	#####	3577	± 26	####
C91215-280.1	###	117	0.63	0.06	######	±	#####	######	±	#####	3089	± 23	####
C91215-281.1	76	45	0.61	0.05	######	±	#####	######	±	#####	3114	± 33	####
C91215-106.1 D	###	607	1.17	3.34	######	±	#####	######	±	#####	1515	± 9	####
C91215-107.1	91	60	0.68	0.14	######	±	#####	######	±	#####	3026	± 30	####
C91215-73.1	###	73	0.55	0.06	######	±	#####	######	±	#####	3069	± 26	####
C91215-74.1	84	62	0.76	0.05	######	±	#####	######	±	#####	3099	± 32	####
C91215-39.1	###	60	0.49	0.03	######	±	#####	######	±	#####	3067	± 27	####
C91215-81.1	###	218	1.60	0.02	######	±	#####	######	±	#####	3371	± 28	####
C91215-502.1	###	160	0.55	0.05	######	±	#####	######	±	#####	3159	± 20	####
C91215-471.1	###	76	0.76	0.04	######	±	#####	######	±	#####	3096	± 30	####
C91215-416.1	###	109	0.67	–	######	±	#####	######	±	#####	3161	± 26	####
C91215-304.1	###	82	0.76	–	######	±	#####	######	±	#####	3040	± 29	####
C91215-534.1	###	113	0.52	–	######	±	#####	######	±	#####	3125	± 22	####

C91215-486.1		91	51	0.58	–	######	±	#####	######	±	#####	3097	± 31	####
C91215-476.1		###	75	0.65	0.01	######	±	#####	######	±	#####	3283	± 29	####
C91215-478.1		71	44	0.64	0.05	######	±	#####	######	±	#####	3163	± 35	####
C91215-560.1	D	###	###	2.03	3.11	######	±	#####	######	±	#####	1199	± 7	####
C91215-541.1		###	63	0.58	0.07	######	±	#####	######	±	#####	3034	± 29	####
C91215-562.1		90	70	0.80	0.08	######	±	#####	######	±	#####	3099	± 31	####
C91215-517.1		###	146	0.72	0.01	######	±	#####	######	±	#####	3254	± 24	####
C91215-277.1		###	142	0.62	–	######	±	#####	######	±	#####	3094	± 22	####
C91215-275.1		68	35	0.53	0.03	######	±	#####	######	±	#####	3135	± 36	####
C91215-323.1		###	119	1.09	0.05	######	±	#####	######	±	#####	3085	± 29	####
C91215-451.1		###	143	1.06	–	######	±	#####	######	±	#####	3086	± 27	####
C91215-372.1		72	38	0.55	0.01	######	±	#####	######	±	#####	3127	± 35	####
C91215-102.1		56	34	0.62	0.03	######	±	#####	######	±	#####	3085	± 38	####
C91215-5.1		###	141	0.53	0.02	######	±	#####	######	±	#####	3108	± 20	####
C91215-103.1		96	62	0.67	0.03	######	±	#####	######	±	#####	3185	± 32	####
C91215-279.1		90	37	0.43	0.06	######	±	#####	######	±	#####	3073	± 30	####
C91215-367.1		81	44	0.56	–	######	±	#####	######	±	#####	3049	± 32	####
C91215-389.1		86	52	0.62	0.03	######	±	#####	######	±	#####	3110	± 32	####
C91215-390.1		80	51	0.66	0.06	######	±	#####	######	±	#####	3117	± 33	####
C91215-369.1		###	136	0.60	–	######	±	#####	######	±	#####	3101	± 21	####
C91215-370.1		###	114	0.83	0.01	######	±	#####	######	±	#####	3086	± 25	####
C91215-375.1		###	121	0.91	–	######	±	#####	######	±	#####	3074	± 26	####
C91215-345.1		###	124	0.56	0.00	######	±	#####	######	±	#####	3120	± 21	####
C91215-346.1		60	36	0.62	0.09	######	±	#####	######	±	#####	3102	± 37	####
C91215-4.1	D	###	###	4.69	4.13	######	±	#####	######	±	#####	1940	± 12	####
C91215-71.1		###	144	0.93	0.01	######	±	#####	######	±	#####	3091	± 24	####
C91215-140.1		47	28	0.61	0.04	######	±	#####	######	±	#####	3127	± 41	####
C91215-250.1		###	213	0.66	0.07	######	±	#####	######	±	#####	2993	± 18	####
C91215-251.1		###	178	1.19	0.07	######	±	#####	######	±	#####	3270	± 26	####
C91215-373.1		97	63	0.67	0.04	######	±	#####	######	±	#####	3110	± 29	####
C91215-388.1		###	122	0.50	0.02	######	±	#####	######	±	#####	3122	± 21	####
C91215-104.1		###	146	0.83	0.03	######	±	#####	######	±	#####	3111	± 23	####

Isotopic ratios are given with 1 σ uncertainties, after the correction for common Pb using the ^{204}Pb correc

Disc. (%) denotes the percentage of discordancy (e.g. Song et al., 1996). D: discordant

/^{206}Pb* (Ma)	Disc. (%)
± 13	4
± 43	50
± 13	6
± 40	56
± 25	24
± 10	9
± 19	13
± 12	5
± 11	0
± 10	42
± 17	-2
± 10	57
± 9	50
± 21	5
± 25	-3
± 16	2
± 16	38
± 12	7
± 26	31
± 26	60
± 12	23
± 11	77
± 11	75
± 17	21
± 13	26
± 11	34
± 15	38
± 5	25
± 26	21
± 26	5
± 16	-7
± 10	21

± 19	3
± 12	-3
± 10	57
± 12	-2
± 11	12
± 12	32
± 12	23
± 11	51
± 10	51
± 18	9
± 12	43
± 10	16
± 30	73
± 10	1

$/^{206}Pb^{*}$ (Ma)	Disc. (%)
± 10	53
± 9	3
± 13	67
± 10	44
± 14	67
± 7	1
± 5	6
± 20	3
± 10	52
± 23	44
± 7	40
± 6	3
± 6	3
± 30	55
± 6	0
± 8	2
± 5	-2
± 9	38
± 9	42

± 9 50

± 8 0

± 10 50

± 13 70

± 6 12

± 18 14

± 5 21

± 8 14

± 8 62

± 8 3

± 18 67

± 7 2

± 7 3

± 8 25

± 17 69

± 36 47

± 8 38

± 7 9

± 9 21

± 12 67

± 6 3

± 11 6

± 12 57

± 6 3

± 9 30

± 6 6

± 6 1

± 7 5

± 10 37

± 9 29

± 8 12

± 10 34

± 7 25

± 8 16

± 10 45

± 9 56

± 6	11
± 11	48
± 10	44
± 8	13
± 9	47
± 10	6
± 7	2
± 8	4
± 9	32

$/^{206}Pb^{*}$ (Ma)	Disc. (%)
± 9	9
± 7	-1
± 12	0
± 13	-2
± 7	1
± 13	-3
± 12	0
± 10	1
± 11	-1
± 7	0
± 7	3
± 13	4
± 9	2
± 7	2
± 11	1
± 42	6
± 10	-2
± 13	2
± 7	1
± 9	0
± 10	-2
± 14	-5
± 11	-3
± 8	0

±	12	0
±	8	0
±	11	6
±	9	-2
±	19	0
±	52	2
±	17	-3
±	31	-1
±	11	-1
±	16	-2
±	10	0
±	9	3
±	11	1
±	9	0
±	12	1
±	7	0
±	8	3
±	6	2
±	23	0
±	13	1
±	8	0
±	8	0
±	12	1
±	14	-1
±	8	-1
±	7	-3
±	12	-1
±	8	-1
±	9	1
±	7	0
±	8	2
±	11	-1
±	7	1
±	8	-3
±	7	0
±	7	-3

± 11	1
± 11	-4
± 12	0
± 9	-1
± 11	2
± 9	-3
± 9	0
± 9	0
± 7	-1
± 9	2
± 12	-3
± 10	2
± 8	0
± 13	-2
± 6	1
± 12	-2
± 8	4
± 14	0
± 9	1
± 8	-1
± 7	0
± 13	2
± 17	-4
± 7	2
± 8	0
± 7	1
± 10	1
± 15	0
± 8	3

$/^{206}Pb^{*}$ (Ma)	Disc. (%)
± 6	5
± 11	2

± 27 -5
± 7 53
± 6 2
± 7 -1
± 8 -3
± 7 0
± 6 2
± 7 0
± 15 4
± 7 0
± 10 -1
± 6 2
± 11 2
± 43 1
± 9 0
± 8 4
± 15 0
± 6 -1
± 6 0
± 7 0
± 9 -1
± 8 0
± 24 -6
± 16 -5
± 6 0
± 17 -2
± 9 -1
± 9 -1
± 6 3
± 5 0
± 6 1
± 9 -1
± 7 0
± 5 0
± 6 2
± 5 1

±	10	-2
±	8	0
±	9	-1
±	16	2
±	7	-1
±	6	1
±	9	0
±	5	0
±	11	0
±	6	-4
±	6	-1
±	8	0
±	6	4
±	6	1
±	8	-2
±	9	1
±	7	1
±	8	3
±	8	47
±	7	26
±	18	-2
±	11	-1
±	5	2
±	6	0
±	10	-2
±	8	61
±	10	2
±	8	1
±	10	0
±	8	0
±	6	3
±	5	-3
±	9	0
±	7	-3
±	38	2
±	6	-2

± 9	0
± 7	1
± 11	-3
± 9	64
± 9	2
± 9	-1
± 6	0
± 6	-1
± 11	-2
± 9	1
± 8	0
± 11	-2
± 12	0
± 5	-1
± 9	-4
± 9	0
± 10	2
± 9	-1
± 10	-1
± 6	0
± 7	0
± 7	1
± 6	-1
± 11	0
± 9	44
± 7	0
± 13	-3
± 5	4
± 6	0
± 9	-1
± 6	-2
± 6	-1

tion method